4-30-2011

# Twin nucleation, twin propagation, twin-slip interactions, pseudo-elasticity, strain-rate sensitivity and non-Schmid's effects of {10¯1 2} twinning in magnesium via in-situ EBSD

Janit Kapil

# TWIN NUCLEATION, TWIN PROPAGATION, TWIN-SLIP INTERACTIONS, PSEUDO-ELASTICITY, STRAIN-RATE SENSITIVITY AND NON-SCHMID'S EFFECTS OF $\{10\bar{1}2\}$ TWINNING IN MAGNESIUM VIA IN-SITU EBSD

By

Janit Kapil

A Thesis
Submitted to the Faculty of
Mississippi State University
in Partial Fulfillment of the Requirements
for the Degree of Master of Science
in Mechanical Engineering
in the Department of Mechanical Engineering

Mississippi State, Mississippi

April 2011

# TWIN NUCLEATION, TWIN PROPAGATION, TWIN-SLIP INTERACTIONS, PSEUDO-ELASTICITY, STRAIN-RATE SENSITIVITY AND NON-SCHMID'S EFFECTS OF $\{10\bar{1}2\}$ TWINNING IN MAGNESIUM VIA IN-SITU EBSD

By

Janit Kapil

Approved:

Haitham El Kadiri
Professor of Mechanical Engineering
(Major Professor)

Mark F. Horstemeyer
Center for Advanced Vehicular Systems
Chair in Computational Solid Mechanics
Professor of Mechanical Engineering
(Committee Member)

Youssef Hammi
Assistant Research Professor
Center for Advanced Vehicular Systems
(Committee Member)

David L. Marcum
Professor of Mechanical Engineering
(Graduate Coordinator)

Sarah A. Rajala
Dean of the James Worth Bagley College of Engineering

Name: Janit Kapil

Date of Degree: April 29, 2011

Institution: Mississippi State University

Major Field: Mechanical Engineering

Major Professor: Dr. Haitham El Kadiri

Title of Study: TWIN NUCLEATION, TWIN PROPAGATION, TWIN-SLIP INTERACTIONS, PSEUDO-ELASTICITY, STRAIN-RATE SENSITIVITY AND NON-SCHMID'S EFFECTS OF $\{10\bar{1}2\}$ TWINNING IN MAGNESIUM VIA IN-SITU EBSD

Pages in Study: 58

Candidate for Degree of Master of Science

*In-situ* EBSD on profuse $\{10\bar{1}2\}$ twinning in magnesium revealed that the twinning stress for nucleation is not totally rate-insensitive but highly dependent on grain boundary misorientation ranging between 10° and 15°. A new regime in the theta-strain curve; Regime-D, before Regime II, was identified for axisymmetric textures and corresponded to mitigation of twin propagation which was markedly rate-sensitive, such when the strain-rate fell below $10^{-5}$/s, twin propagation, but not twin nucleation, was completely halted and this fact substantiates the predominant effect of transmutation on Regime II hardening over that of Hall and Petch by twin segmentation. This technique revealed that twin nucleation dominates twin growth rate over twin propagation in grains undergoing multi-variant twinning under high-Schmid factors. Pseudo-elasticity in Mg was revealed to originate from an unusual detwinning phenomenon of residual twins. This effect was attributed to incomplete accommodation slip necessary for the shape change by twin to take place.

Keywords: In-situ EBSD, Non-Schmid's effects, grain misorientation, strain-rate dependence, twin nucleation, twin propagation, pseudo-elasticity, twin-twin hardening

DEDICATION

I would like to dedicate this research to my family and friends who supported me in every aspect of my life.

ACKNOWLEDGEMENTS

I would like to express my sincere gratitude to my advisor Dr. Haitham El Kadiri who introduced me to the world of material characterization along with his support, technical guidance and motivation, without which this research could not have materialized. I would also like to thank my committee members Dr. Mark Horstemeyer, who has been an inspiration throughout my entire graduate program and Dr. Youssef Hammi, who always helped me in my needs. Expressed appreciation is also due to Dr. Andrew Oppedal who always guided me throughout my work, Mr. Crawford Baired who helped me in learning various tools for my research, Ms. Melissa Mott and Mr. Stephen Horstemeyer.

I would also like to thank Mississippi State University's Center for Advanced Vehicular Systems, James Worth Bagley College of Engineering and Department of Energy for their financial support and for providing me all the resources used during my research.

TABLE OF CONTENTS

LIST OF TABLES

LIST OF FIGURES

# CHAPTER I

# INTRODUCTION

The most prominent and rigorous experimental investigations on the mechanisms behind the effect of twin nucleation and twin propagation on strain hardening concerned primarily single-lattice metals represented by face-centered cubic (FCC) and body-centered cubic (BCC) structures. These experimentations were mostly performed in between the nineteen fifties and the nineteen seventies. That is, relatively little attention was given to twinning stress and twin propagation in the hexagonal close-packed (HCP) metals despite their ability to develop a much more prolific twinning than in FCC, BCC and cubic structures in general (Meyers et al. 2001). In the last past two decades, however, a vast interest emerged on the fundamental behavior of HCP structures due to the essential role they could play in reducing green house emission and in promoting nuclear energy (Joost 2010).

## 1.1 Twin Nucleation

In early works, twin nucleation was the most favored topic. In fact, the twinning threshold stresses exhibited a puzzling dependence on the microstructure, strain rate, temperature, stress state, and texture. Efforts were directed to formally understand these effects so that rigorous incorporations at higher scales such as crystal plasticity could be possible. The experimental results were, however, substantially divergent, fact that

various review papers and theoretical attempts to put forward a reconciling mechanism (Christian & Mahajan 1995; Mahajan & Williams 1973; Reed-Hill 1973; Venables 1964a; Meyers et al. 2001; Cottrell & Bilby 1951; Bolling & Richman 1965a; Hirth 1964; Sleeswyk 1974). A large number of authors attributed the scatter to the state of pre-existing defects in the crystals, which seemed to highly promote twin nucleation (Price 1960b; Price 1961a; Price 1961b). As such, the Schmid's law should in principal be still applicable to twinning (Thompson & Millard 1952; Allen et al. 1956; Cox et al. 1957; Reid et al. 1966), but with a marked sensitivity to material impurity. This motivated some authors to believe that twin embryo always accidently pre-existed in the investigated samples (Christian 2002b), and it would be a stopped-elastic twin in Garber's notation (Cahn 1953b; Cahn 1953a). Otherwise, twins originate either from spontaneous nucleation under the elastic field induced by stress and promoted by internal defects (Price 1961a; Price 1960a; Bell & Cahn 1953; Price 1961b), or from dissociations of slip dislocations (Mendelson 1970; Mendelson 1969; Mendelson 1970; Mendelson 1969; Mendelson 1969). The three above mechanisms for twinning nucleation are still a matter of strong debates.

In general, literature tended to ascribe an athermal characteristic to twin nucleation, but this was mostly based on observations in FCC structures. Actually, even for FCC structures, authors like Narita and Takamura (1974) observed a positive-temperature dependence of twinning stress in stage III. Mahajan and Williams (1973) agreed on this dependence for FCC but suggested the opposite for BCC. However, Reed-Hill (1973) considered the negative-temperature dependence reported by Mahajan and Williams (1973) as apparent because of the substantial slip concomitant to twinning.

Based on results by Bolling and Richman (1965a; 1965b; 1965c), Reed-Hill (1973) generalized the positive-temperature sensitivity of twinning stress to BCC structures. It is important to note that these studies used materials for FCC and BCC that differed substantially in terms of the stacking fault energy (SFE). Venables (Venables 1964b; Christian 2002c) and Narita and Takamura (1992) emphasized the effect of SFE on twinning stress for many FCC alloys.

There are no rigorous experimental reports on the effect of temperature on the twinning stress in HCP metals. Most tests performed at high temperatures concerned polycrystals with little care paid to prohibit slip and isolate the sensitivity of twinning stress.

The twinning stress sensitivity to strain rate was more readily acceptable in literature than that to temperature. However, the range of strain-rate where a noticeable effect could be detected reached the dynamic regime (up to 1000/s) (Harding 1967; 1968; 1969). Authors normally agreed upon a negative strain-rate dependence for BCC, FCC and even HCP materials such as zirconium (Zr) (Reed-Hill 1973; Harding 1969; Harding 1967; Harding 1968). Regarding this effect, again, little attention was paid to isolate the effect on twinning in HCP structures. However, recent literature suggests that a ubiquitous combination of temperature and strain rate may exist for profuse $\{10\bar{1}2\}$ twinning as long as temperature is noticeably below the melting temperature (L. Li et al. 2006; Jain & Agnew 2007). However, this effect is still to be confirmed experimentally. In general, literature seems to believe that twin enhancement by strain rate stems actually from the hardening of slip to a level the thresholds stress of non-<a>

basal dislocations exceeds a probably rate-insensitive $\{10\bar{1}2\}$ twinning stress, thereby allowing twinning to kick in easier (Jain & Agnew 2007).

## 1.2 Twin Propagation

There are two stages of twin propagation that stem from different mechanisms, namely the catastrophic lengthwise thickening parallel to the composition plane and the progressive edgewise thickening normal to the habit plane, known as normal growth or twin propagation (Christian 2002a). The lengthwise thickening has strong ties with nucleation (Wang et al. 2009) and involves complex mechanisms related to formation of emissary dislocations and to elasto-plastic compatibility at the tip of the tapering twin ((Sleeswyk 1962; Votava & Sleeswyk 1962; Mahajan 1975). These complexities transcend the scope of this introduction. However, accommodation effects by slip and kinking are of considerable importance for the reversibility of the twin whether by stress removal or stress reversal. The twinning shear is either accommodated by elasticity in the matrix or by slip or kinking, usually in the matrix (Pratt & Pugh 1952; Pratt & Pugh 1953). The idea that a twin accommodates plastic deformation without kinking or slips in the matrix is erroneous, although it had dangerously spread in recent literatures. The ability of matrix slip under twinning has a fundamental effect on detwinning, and, as it will be shown in this paper, on Pseudo-elasticity.

The twin propagation is a widely discussed topic in the literature, but the fundamentals were primarily provided between the nineteen fifties and the nineteen seventies. Starting from the nineteen eighties, most efforts concentrated on numerical investigations of the previous theories through atomistic simulations (Serra & Bacon

1996; B. Li & Ma 2009a; Serra & Bacon 1995; Serra et al. 1991; Serra & Bacon 1986; Serra et al. 2002; B. Li & Ma 2009b).

A crucial topic concerned the origin and dynamics of twinning disconnections that accommodate normal growth. Theoretical efforts led to two distinct schools of thought.

The first school assumed spontaneous nucleation of twinning disconnections, whereupon stress and thermal agitation act in tandem to create little islands of twin on each successive lattice composition plane. Confounding the elastic properties of the matrix and the interface, the theory implied that a nucleation would be improbable if the Burgers vector magnitude of the twin disconnection exceeds approximately one half of the interatomic spacing in the composition plane. This ramification was consistent with twin propagation in double-lattice structures such as face-centered tetragonal, orthorhombic and $\{10\bar{1}2\}$ twinning in HCP, but inconsistent with twin propagation in cubics. However, based on the wider core of twinning disconnections compared to bulk dislocations (Bristowe & Crocker 1977; Yamaguchi & Vitek 1976), Yamaguchi and Vitek (1976) provided calculations that corroborated the normal growth by spontaneous nucleation, and actually supported the fact that the twinning stress for growth is a fraction of that for nucleation. In sum, there is so far no theory put forward that would negate the theory of spontaneous nucleation for twin propagation.

However, the most widely accepted theory for twin propagation is the pole mechanism for normal growth put forward independently by Cottrell and Bilby (1951) and Millard and Thompson (1952). This theory rests on the creation of generating nodes and twinning disconnections by matrix slip dislocations when they intersect the twin

boundary. The dislocation segment within the matrix, respectively within the twin, and connected to the node, forces the gliding twinning disconnections to proceed forward toward the matrix, resp. or backward toward the twin, accommodating normal twinning growth, resp. normal detwinning shrinkage depending on the stress sign. The theory showed a remarkable consistency with the fact that twinning stress for growth is a fraction of that for nucleation (Cottrell & Bilby 1951).

### 1.3 Pseudo-elasticity

Pseudo-elasticity was first discovered by Reed-Hill et al. (1965) at room temperature in Zr samples pre-strained at liquid nitrogen temperature. The mechanical hysteresis was attributed to $\{11\bar{2}1\}$ movements, as it was largely affected by stress but only slightly by strain rate. C áceres and co-workers (Cáceres et al. 2003; Muránsky et al. 2009; Mann et al. 2007) confirmed the effect of twinning on pseudo-elasticity by partial reversibility of $\{10\bar{1}2\}$ lamellae upon stress removal. This effect would have strong commercial significance in springback upon forming by superplasticity (Reed-Hill et al. 1965).

### 1.4 Microstructure and Non-Schmid's Effects

A good amount of attention was given to HCP structures regarding the effect of grain size on twin nucleation compared to that for cubic. The negative-grain size dependence observed in FCC and BCC was found to be even more pronounced in HCP structures. Following the grounds of micro-plasticity suggested by Vöhringer (1976)and Armstrong and Worthington (1973), Meyers et al. (2001) developed a dislocation pile-up

based constitutive model with a critical review of the literature, to account for this effect. The idea was based on the primarily role of pile-up on twin nucleation. If the grain size does not allow the dislocations to pile-up along a sufficiently long segment, then the twinning stress would not be reached, and simply, the twin won't nucleate. This theory could be qualified as questionable as it will be demonstrated in this paper.

Recent literature pointed to non-Schmid's effect due to the back-stress arising from the incompatibility at the grain boundary where the residual twin lamella impinges (Wang et al. 2009; Martin et al. 2010; Capolungo et al. 2009; Beyerlein et al. 2010). These works were primarily inspired by previous observations carried out by Mahajan on accommodation effects and twin-twin interactions Mahajan and Chin (1973).

The grain boundary misorientation effects on twin nucleation is one the most distinguished contributions of recent literature. This will be clearly illustrated in this paper via in-situ EBSD. Low misoriented tilt boundaries would promote substantially twinning (Beyerlein & Tomé 2010; Beyerlein et al. 2010; Wang et al. 2010). These observations were incorporated in a crystal plasticity framework (Beyerlein & Tomé 2010; Beyerlein et al. 2011).

Particles could promote or prohibit twinning as interstitials do (Robson et al. 2010; Stanford et al. 2009). The effects are still obscure but could be linked to shuffling.

This paper investigates the mechanisms of twin nucleation, twin propagation, pseudo-elasticity and non-Schmid's effect in magnesium via non-destructive electron backscattered diffraction (EBSD) performed on the same region undergoing deformation. EBSD is a powerful technique that allows texture analysis at the sub-micron scale.

However, most EBSD studies on profuse magnesium were carried out with destructive EBSD techniques that did not enable to follow the evolution of a same physical twin.

To appreciate the effect of grain size and misorientation effect on twin nucleation and propagation in the *same sample* an AM30 Mg alloy was prepared so it shows separate clusters of small grains and large grains, with grain misorientation ranging from few degrees to 180°. This type of microstructure was accessible by controlled extrusion which allowed small dynamically recrystallized grains and large parent grains including boundaries with misorientations from few degrees to 20°. The extrusion parameters were also controlled to obtain a homogeneous axisymmetric texture so the Schmid factor for twinning would be high for almost all grains upon compression normal to the axis of the axisymmetric texture component ring, which corresponded to the extrusion direction (ED).

CHAPTER II

MAGNESIUM ALLOYS

## 2.1 History and Advantages of Magnesium Alloys

Magnesium is the seventh most abundant element in the Earth's crust. Magnesium comprises 0.13% of the ocean water providing a tremendous source for the metal (Avedesian and Baker, 1999, Mordike, B.L., Ebert, T., 2001). In the past, magnesium was used extensively in World War I & II as in nuclear, military, and German military aircraft applications. Various automakers like Mercedes Benz, BMW, and Porsche used magnesium alloys for engine blocks, wheels, body panels etc. The most significant application was its use by German Automaker Volkswagen. The Volkswagen Beetle automobile is probably the largest single application using a magnesium alloy in its engine components. Magnesium is the lightest structural metal and can be used in wide range of applications where light weight is of significant advantage. This property attracts automobile manufacturers to replace heavy materials like steel, cast iron and even aluminum alloys by magnesium based alloys. Magnesium alloys are either cast or wrought alloys but wrought alloys seems to have better mechanical properties as compared to cast alloys due to the defects in cast alloys like porosity, inclusions and low ductility (Wang, Y.N., Huang, J.C, 2007 ). The major problems encountered in wrought components are the poor workability and strong directionality of properties which seems

to be caused by the particular deformation characteristics of the hexagonal crystal structure.

Though a number of wrought magnesium alloys like AZ31, AZ61 etc. have already been used in the previous studies, now a new wrought magnesium alloy AM30 has been developed and is used in this study. Aluminum has the most favorable effect on magnesium as it improves strength and hardness. An Aluminum content of about 5-6% yields the optimum combination of strength and ductility for structural applications (Luo, A., Alan, Sachdev, Anil, K., 2007). Therefore, an aluminum content of 3% was selected to improve ductility and extruability while maintaining reasonable strength and castability. Manganese increase yield strength of magnesium alloys slightly along with improving corrosion resistance of Mg-Al based alloys by removing iron and other heavy metal elements. So, for this purpose, Mn is added at about 0.4% as recommended by the ASTM specification B93-94a. Therefore, based on these analysis and some preliminary experiments a new magnesium alloy AM30 (Mg-3% Al-0.4%Mn), was developed to provide a good balance of strength, ductility, extruability and corrosion resistance. The chemical composition in weight (%) of magnesium alloy AM30 is shown in Table 3.1.

## 2.2 Deformation Mechanism in Magnesium

Magnesium has a hexagonal lattice structure with lattice parameters a1=a2 ≠ c as a = 3.2Å, c = 5.2Å and c/a = 1.623 (as described by Partridge P.G.) as shown in Figure 2.1. Where a, denotes the inter-atomic distance and c, is the height of the unit cell in the c-direction. These parameters greatly defines the fundamental role of magnesium and its

alloys and also differentiate it from face-centered cubic (FCC) and body-centered cubic (BCC) structures.

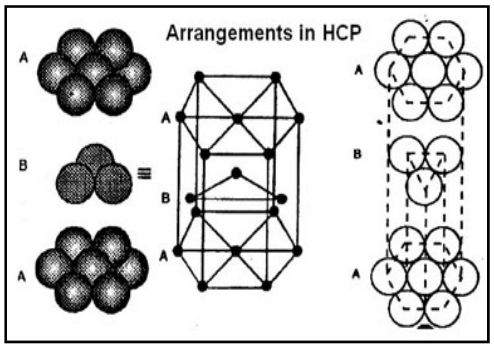


Figure 2.1 Hexagonal Close-Packed (HCP) structure describing the position of atoms

Plastic deformation of hexagonal lattice is more complicated than cubic latticed metals like aluminum, copper or steels due to their inherent anisotropy that result from their crystallographic structure. Deformation behavior of magnesium is described in number of studies by the limited number of slip systems of its hexagonal close-packed crystal structure (Kelly, E.W., Hosford, W.F., 1968). Taylor proposed that five independent slip systems are required to undergo a general homogeneous deformation, without producing cracks, for a polycrystalline material, based on Von Mises criterion (Yoo, M.H., 1981). The slip systems, described using the Miller-Bravais system's four indices (Otte and Crocker) are shown in Figure 2.2. In FCC metals, plastic deformation occurs easily as the required five slip systems are present in one family but, in HCP-structured metals simultaneous activity of primary and secondary slip and twinning mechanisms must interact to allow plastic deformation (Kocks and Westlake, 1967, Agnew et al., 2003, 2006; Keshavarz and Barnett, 2006). At room temperature, the most

easily activated deformation mode is $(0001)<11\bar{2}0>$ basal slip which is the primary slip system. Prismatic slip $\{10\bar{1}0\}<11\bar{2}0>$ and pyramidal slip $\{10\bar{1}1\}<11\bar{2}0>$ have also been reported in magnesium at high temperatures (Zhang, Shaorui, Peng, Yinghong, Tang, Weiqin, Li, Dayong, 2009).

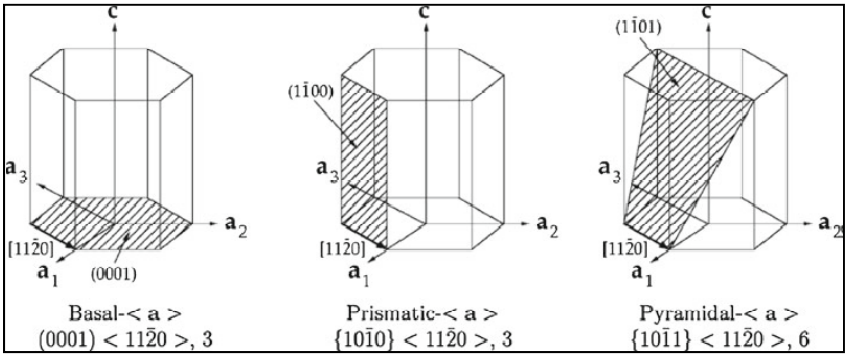


Figure 2.2 Schematic of deformation modes: Basal-<*a*>, prismatic-<*a*>, and pyramidal-<*a*> slip systems of HCP materials.

According to the measured data, the reason for easy activation of basal slip at low temperature is the lower value of the critical resolved shear stress while the critical shear stress values for other slips systems are comparatively high at these temperatures (Seong et al, 2010, Koike, J., 2005).

Kocks and Westlake (1967) first noted that the presence of mechanical twinning in some hexagonal close-packed (HCP) metals, such as magnesium, modifies the slip situation by essentially requiring other independent deformation modes. Since the limited slip on basal planes provide only two independent slip systems, fewer than the necessary five independent slip systems for homogeneous deformation, the limited slip system result in poor formability of hexagonal close-packed metals (Seong-Gu Hong, Sung

Hyuk Park, Chong Soo Lee, 2010, Koike, J., 2005). Considering the prismatic slip along with the basal slip to accommodate the requirement but together these two systems provide only four independent systems on which slip can occur. Therefore, mechanical twinning provides the required fifth mode for proper deformation of a polycrystalline material satisfying the Von-Mises criteria.

## 2.3 Deformation Twinning

The classic definition of twinning signifies that the twin and parent (or matrix) lattices are related either by a reflection in some plane or by a rotation of 180˚ about some axis. It is a process in which two or more crystals, or parts of crystals, assume orientations such that one may be brought to the coincidence with the other by reflection across a plane or by rotation about an axis (Christian, J.W., Mahajan, S., 1995) as shown in Figure 2.3. The parent lattice is re-oriented by atom displacements which are equivalent to a simple shear of the lattice points and this shear plane is termed as $K_1$ and corresponding shear direction is termed as $\eta_1$ (intersection between $K_1$ and the plane of shear). The second invariant plane by shear is $K_2$ while the intersection between $K_2$ and the plane of shear is $\eta_2$ where x3 is the normal to $K_1$.The twinned region of the lattice becomes a mirror image of the untwined region. This method of deformation is common in low symmetry crystals like hexagonal close-packed materials where the sufficient number of slips systems required for general deformation may not be available. The tendency of a crystal to twin is largely depend on its c/a ratio. The ideal c/a ratio for twinning to occur is around ~ 1.623, which is the value for magnesium.

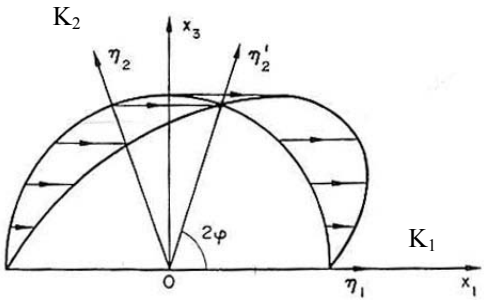


Figure 2.3 Schematic illustration of deformation twinning elements. The twinning and conjugate twinning planes are $K_1$ and $K_2$ while their corresponding directions are $\eta_1$ and $\eta_2$.

Since twinning is Polar in nature (Christian, J.W., Mahajan, S., 1995), twinning modes can either accommodate strain along tensile direction or compressive direction thereby exhibit two types of twinning modes, (a) Tension twins (b) Compression twins. The most common twinning mode reported in magnesium is tension twinning, $\{10\bar{1}2\} < \bar{1}011>$ (as shown in Figure 4) (Lee et al, 2010, Zhang et al, 2009).

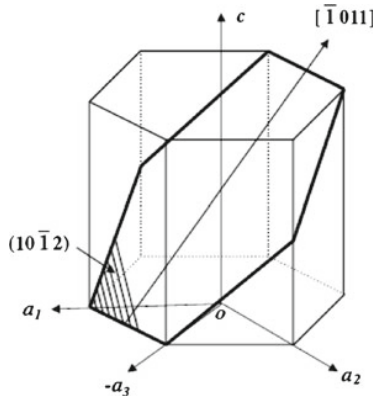


Figure 2.4 Schematic illustration of $\{10\bar{1}2\} < \bar{1}011>$ tension twinning system for the magnesium's hcp crystal structure.

It is relatively easily activated by tension parallel or compression perpendicular to the c-axis. Twinning is polar in nature i.e. The polar characteristics of twinning only allow it to take place in one direction of deformation, and this direction is determined by the c/a ratio. Thus magnesium can deform by $\{10\bar{1}2\}$ twinning (referred as "Tension Twins") when stressed by tension along the c-axis and by $\{10\bar{1}1\}$ twinning (referred as "Compression Twins") when stressed by compression along the c-axis (Kelly, E.W., Hosford, W.F., 1968). In addition to the primary twinning, secondary twinning or slip can also occur within the reoriented crystal. In the case of tension along the c-axis, the basal plane is reoriented by twinning nearly 90˚ from one position to another. Also, before twinning the c-axis is perpendicular to the loading direction but after twinning it is nearly parallel to it (Barnett, M.R., 2007a). This reorientation caused by twinning can have an effect on work hardening behavior and may have both hardening and softening effects. The existence of work hardening is assumed because of the twin boundaries that may act as barriers to dislocation motion, like grain boundaries, leading to increase the hardening rate while the accommodation of strain along c-axis may reduce the work hardening rate (Muransky, O.; Carr, D.G.; Sittner, P.; Oliver, E.C., 2009, Wang et al, 2007). In case of highly textured magnesium, majority of crystals are oriented preferably due to which twinning occurs only in one direction and not in other and this unique one directional characteristics of twinning makes the designing of magnesium components more challenging. It is also reported that different twin variants can operate depending on the direction of strain applied (Agnew, S.R., Yoo, M.H., Tome, C.N., 2001, Barnett, M.R., 2007a). The factors including initial texture, grain size, strain path and temperature have a great influence on twinning behavior.

## 2.4 Brief History of Experimental Work

Magnesium alloys are extensively employed in many applications due to their excellent physical properties such as low density, high specific strength and high stiffness but they are historically recognized as a metal with poor formability at room temperature due to their less symmetric hcp structure. Initial research of magnesium's deformation characteristics was determined mainly by the experimental work conducted during early 1950s and 1960s. Roberts, (1960), suggested the fact that the unavailability of five independent slip systems to satisfy the Taylor criterion leads to strong anisotropy and thereby decreasing the formability of magnesium alloys. Kocks and Westlake (1967) first noted that the presence of mechanical twinning in some hexagonal close-packed (HCP) metals, such as magnesium, modifies the slip situation by essentially requiring other independent deformation modes. Kelly and Hosford (1968) discovered that polycrystalline magnesium becomes more anisotropic as it becomes more textured. Slip and Twinning show a strong sensitivity to changes in the initial texture, temperature, microstructure, loading path, strain rate, stress state (Yoo, 1981; Thornburg and Piehler, 1975; Partridge, 1967; Christian and Mahajan, 1995). In mid 20s, a number of studies were conducted on hcp metals like AZ31, AZ61, Zr, Ti, on the effect of strain rate, strain path, orientation, grain size, texture on deformation twinning and thereby its effects on various properties but nothing much had been done on twin morphology till then. Recently, a major study has been conducted on twin nucleation and twin growth in hexagonal close-packed structures by Capolungo, L., Beyerlein, I.J, Tome, C.N., Wang, L., (2008, 2009 and 2010).

CHAPTER III

# TWIN NUCLEATION, TWIN PROPAGATION, TWIN-SLIP INTERACTIONS, PSEUDO-ELASTICITY, STRAIN-RATE SENSITIVITY AND NON-SCHMID'S EFFECTS OF $\{10\bar{1}2\}$ TWINNING IN MAGNESIUM VIA IN-SITU EBSD

## 3.1. Experimental Procedure

### 3.1.1 Material and Microstructure

The chemical composition of the material employed in this study, which was an extruded magnesium alloy AM30 is presented in Table 3.1. All the investigated samples were extracted by electrical discharge machining (EDM) in the form of cubes of 6mm side so to enable analyzing by EBSD a flat section parallel to the compression axis (Figure 3.1.a). Three Regions, namely Region A(R-A), Region B(R-B), Region C(R-C) were selected for EBSD analysis at each increment of 0.05% strain (Figure 5a).

Table 3.1 Chemical composition (in wt. %) of Magnesium alloy AM30

| Al | Mn | Zn | Fe | Si | Cu | Ce | Ni | Mg |
|---|---|---|---|---|---|---|---|---|
| 2.54 | 0.40 | 0.018 | 0.003 | 0.008 | 0.011 | 0.025 | 0.005 | Bal. |

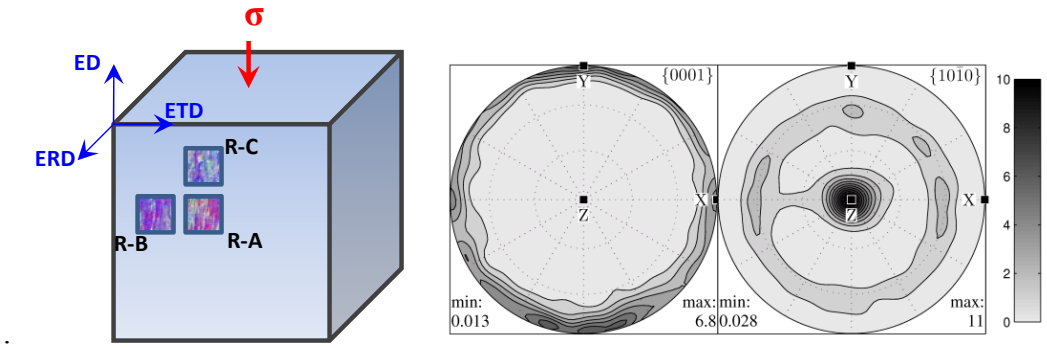


Figure 3.1 (a) A schematic illustration of the sample geometry compressed along extrusion direction (ED) and scanned with EBSD on a section normal to (ERD) over three regions, namely R-A, R-B and R-C. (b) Complete [0001] and [10$\bar{1}$0] pole figures obtained by neutron diffraction data revealing an axisymmetric texture realized by recrystallized grains having a spread around the ED|| [2$\bar{1}\bar{1}$0] and parent grains having a spread around ED||[10$\bar{1}$0].

As mentioned in the last paragraph of the introduction, the extrusion of AM30 was controlled to generate a mixed grain microstructure composed of clusters of small grains and clusters of large grains. The clusters of small grains originated from dynamic recrystallization (DRX) during extrusion as revealed by the grain orientation spread map (Figure 3.2.c). These clusters internally offered a homogeneous distribution of grain boundary misorientation (Figure 3.2.c). The large grain clusters corresponded to parent grains, and offered rather a low average misorientation distribution with a spike at approximately 10° (Figure 3.2.c). The parent grains are 1/3 of dynamic recrystallized grains (DRX) show a spread around ED||[10$\bar{1}$0] component, while 2/3 of the DRX grains exhibited a spread around ED|| [2$\bar{1}\bar{1}$0] component. The volume fraction of dynamic recrystallized grains being approximately twice that of the parent grains, the overall texture developed a prismatic-ring with relatively uniform distribution (Figure 3.1.b).

Interrupted tests at plastic strains starting from 0.3% to 8.5% plastic strain were performed on the same sample along the extrusion direction (ED) to analyze the evolution of deformation texture and twinning. The sample for microscopy and EBSD examination was prepared by first polishing the sample with Silicon carbide paper of different grits followed by the smooth polishing with different cloths using a solution of ethylene glycol and various grits (3m, 1μm, 0.25 μm) of alumina followed by subsequent etching with the solution of Nitric acid and water. All microstructure calculation and analysis were conducted by using an Electron Back-Scattered Diffraction (EBSD) technique from a Zeiss Supra-40 FEG-SEM equipped with a TSL OIM data acquisition and analysis software package. A voltage of 23 KV and CI >0.1 was chosen during the acquisition of EBSD data. Two samples were tested to quantify the nucleation of twins after the first initial deformation.

The inverse pole figure maps of AM30 obtained by EBSD for sample 1 and sample 2 along ED direction are presented in Figure 3.2.(a) and (b). The initial texture of AM30 measured by neutron diffraction in Los Alamos National laboratory (S. Vogel) along with the information on the microstructural characteristics of the material are presented in Figure 3.1(b) and Figure 3.2.

EBSD analysis showed large elongated grains in the extrusion direction and small equiaxed grains located at the grain boundaries of the large elongated grains. The grain orientation spread shows that the large elongated grains are parent grains (33%) that underwent substantial deformation along extrusion direction and the equiaxed grains are recrystallized (DRX) grains (66%) as shown in Figure 3.2 (d), (e).

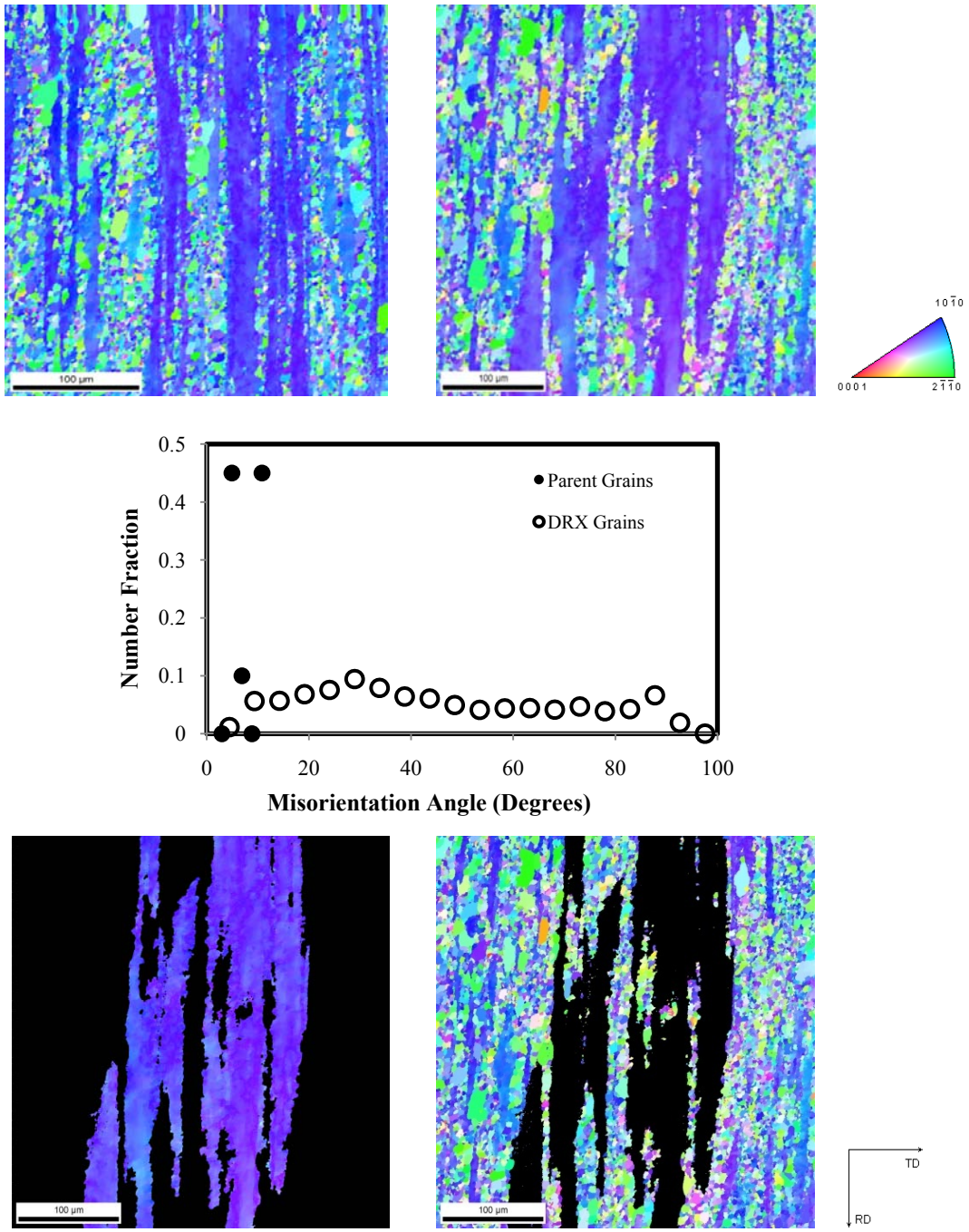


Figure 3.2 Inverse pole figure maps of an extruded AM30 magnesium alloy obtained by EBSD along extrusion direction (ED) for (a) sample 1 (b) sample 2(c). Misorientation distribution of parent grains and dynamic recrystallized grains (marked as DRX) obtained by EBSD and shows a uniform distribution in the DRX grains up to 90˚ and a spike in the parent grains at approximately 10˚. (d) Large elongated parent grains in blue are 33% and (e) small DRX grains in green are 66% of the total area.

The AM30 Mg alloy was extruded at relatively high temperatures of 570˚C and at an extrusion speed and ratio of 0.046 m/s and 6.25, respectively. The initial texture of the material showed an intense basal texture with most basal planes aligned parallel to the extrusion direction. It can be seen that the c-axis is distributed perpendicular to the extrusion direction. The material had a twin free grain structure with an average grain size of 20 μm for sample 1 and 28 μm for sample 2.

### 3.1.2 Mechanical Testing

The quasi-static compression true stress vs. true plastic strain behavior and strain hardening rates (Theta) at room temperature for strain rates of $10^{-5}s^{-1}$, $10^{-3}s^{-1}$ and $10^{--1}s^{-1}$ along extrusion (ED) direction are presented in Figure 3.3. The compression carried out perpendicular to the c-axis (or followed by amount of extension along the c-axis). The true plastic stress-strain behavior along ED direction exhibit a sigmoidal- shaped flow curve which is known to be a typical feature of twinning dominated deformation (Barnett, M.R., et al, 2004, Jiang, et al, 2006, 2008, Knezevic, et al, 2010). It can be assumed that, although the early deformations (<~ 6%) under all the strain rates were dominated by the same $\{10\bar{1}2\}$ twinning, their deformation characteristics were different from each other. A slight difference in the yield stress is observed in all the strain rates but a vast difference is observed in the strain hardening rate curves for all the strain rates. These differences in deformation characteristics emerge from the difference in $\{10\bar{1}2\}$ twinning characteristics, which are dependent upon strain path.

### 3.1.3 Twin Morphology

The evolution of twin morphology with different strains along ED is presented in Figure 3.4. All the experimentation and microstructure analysis were conducted on sample 2 for further consideration. Three regions were selected as shown in Figure 3.1(a) and marked as Region A, Region B and Region C, were measured by means of EBSD and different twin morphologies was observed in them. The first appearance of twins was observed at 1.3% plastic strain as shown in Figure 4.3. Region A has three substantial parent grains having increasing area out of which the largest parent grain has been considered for analysis and is named as Grain1. Regions B shows two substantial parent grains of different twin morphology and are named as Grain 2 and Grain 3. Region C shows one major parent grain and is named as Grain 4. Figure 3.4 shows inverse pole figure (IPF) maps for four stages of deformation namely 2.8%, 4.7%, 6.5% and 7.9% plastic strain. The most common feature between these IPF maps is the substantial growth of $\{10\bar{1}2\}$ $<10\bar{1}1>$ extension twin. Volume fraction of twins is calculated directly using the pole figures with the help of OIM analysis software by manual selection of orientations falling within the range of 35˚ tolerance. As seen that the twins dominates and covers almost all the parent grains at the end of the deformation.

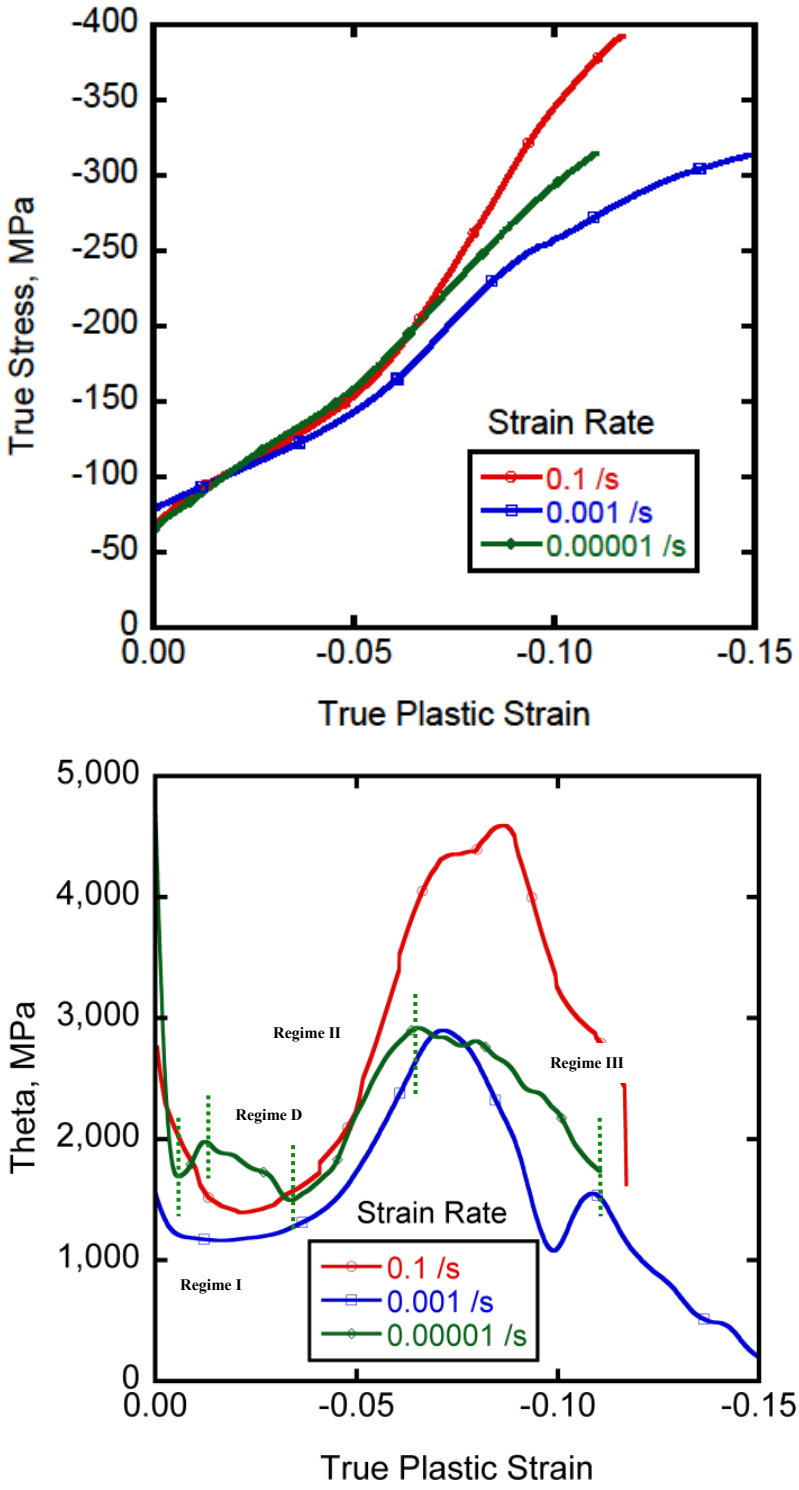


Figure 3.3 Deformation characteristics along extrusion direction (ED) at $10^{-5}s^{-1}$, $10^{-3}s^{-1}$ & $10^{-1}s^{-1}$ (a) stress-strain curve and (b) strain hardening rate curve. A new Regime D is observed clearly at $10^{-5}s^{-1}$ in strain hardening rate curve as shown in green color, in comparison to all the other strain rates.

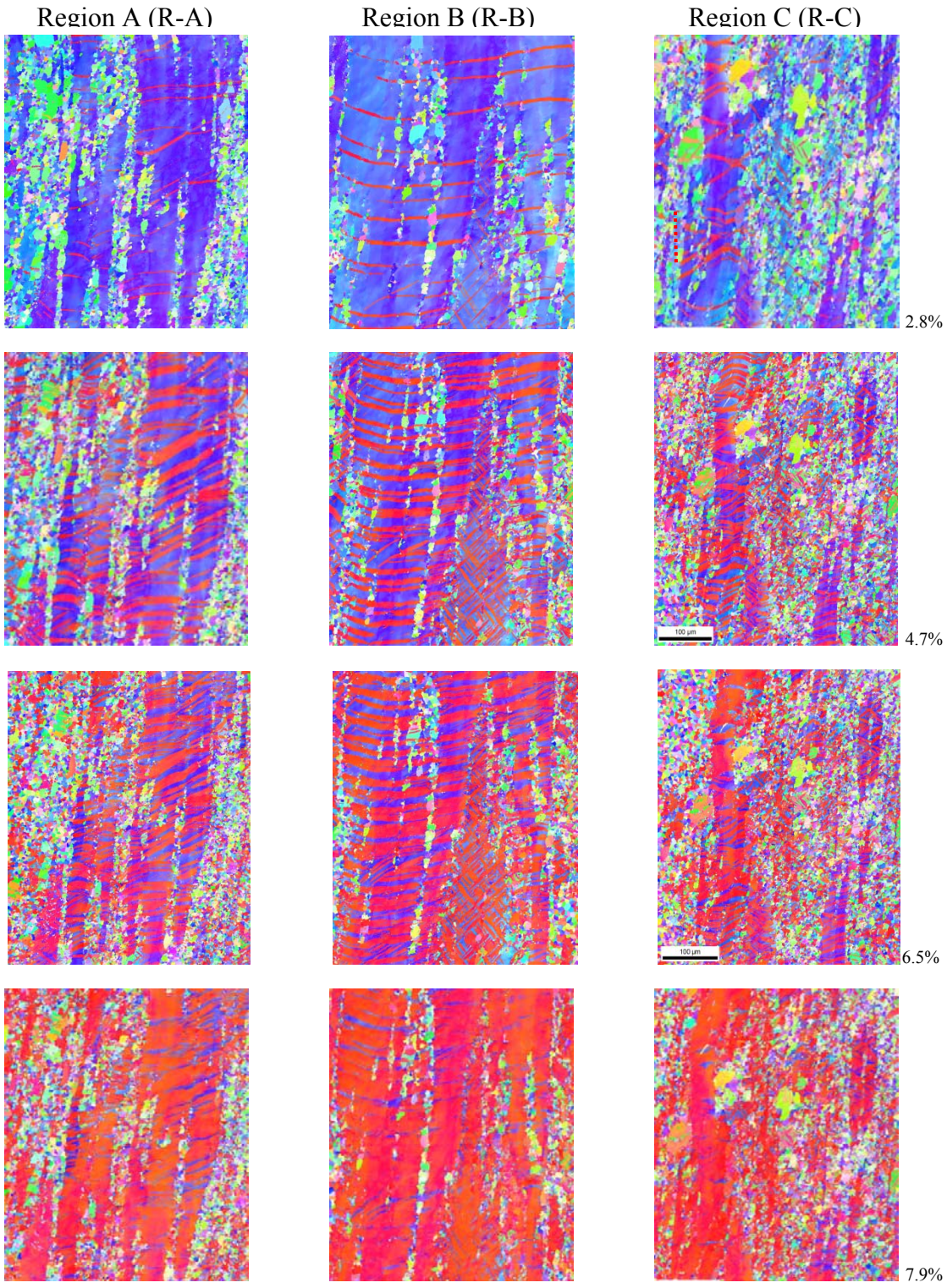


Figure 3.4 IPF maps obtained by EBSD for Region A, Region B, Region C at 2.8%, 4.7%, 6.5% and 7.9% plastic strain exhibit different twin morphologies. Twins evade the whole area as deformation reached 7.9%. Region B shows two grains with different twin variants active.

CHAPTER IV

RESULTS AND DISCUSSION

## 4.1 Effect of Grain Boundary Misorientation on Twinning

### 4.1.1 Effect of Texture on Threshold Stresses of Twinning and Slip

To observe the effect of texture on threshold stresses of twinning and slip, we studied two textures for the same material, magnesium alloy AM30, axisymmetric extrusion texture and plane strain extrusion texture, developed using neutron diffraction at Los Alamos National laboratory by S. Vogel as shown in Figure 4.1. The axisymmetric texture is achieved with the help of recrystallized grains. All the blue grains corresponds to ED//$(10\bar{1}0)$ while all the green grains corresponds to ED//$(2\bar{1}\bar{1}0)$ plane. Corresponding EBSD inverse pole figure maps were measured for these two initial textures followed by the compressive and tensile deformation of both textures along extrusion direction (ED) and extrusion transverse direction (ET). The curve shows profuse twinning along ED direction and parabolic response along ET direction during compression for axisymmetric texture. The important thing to notice here is the difference in yield points for both the textures. Crystal plasticity dislocation based model was used to simulate the experimental curves for both the textures. An interesting point we observed here is that the crystal plasticity model revealed different results for both the textures as shown in Figure 4.2.

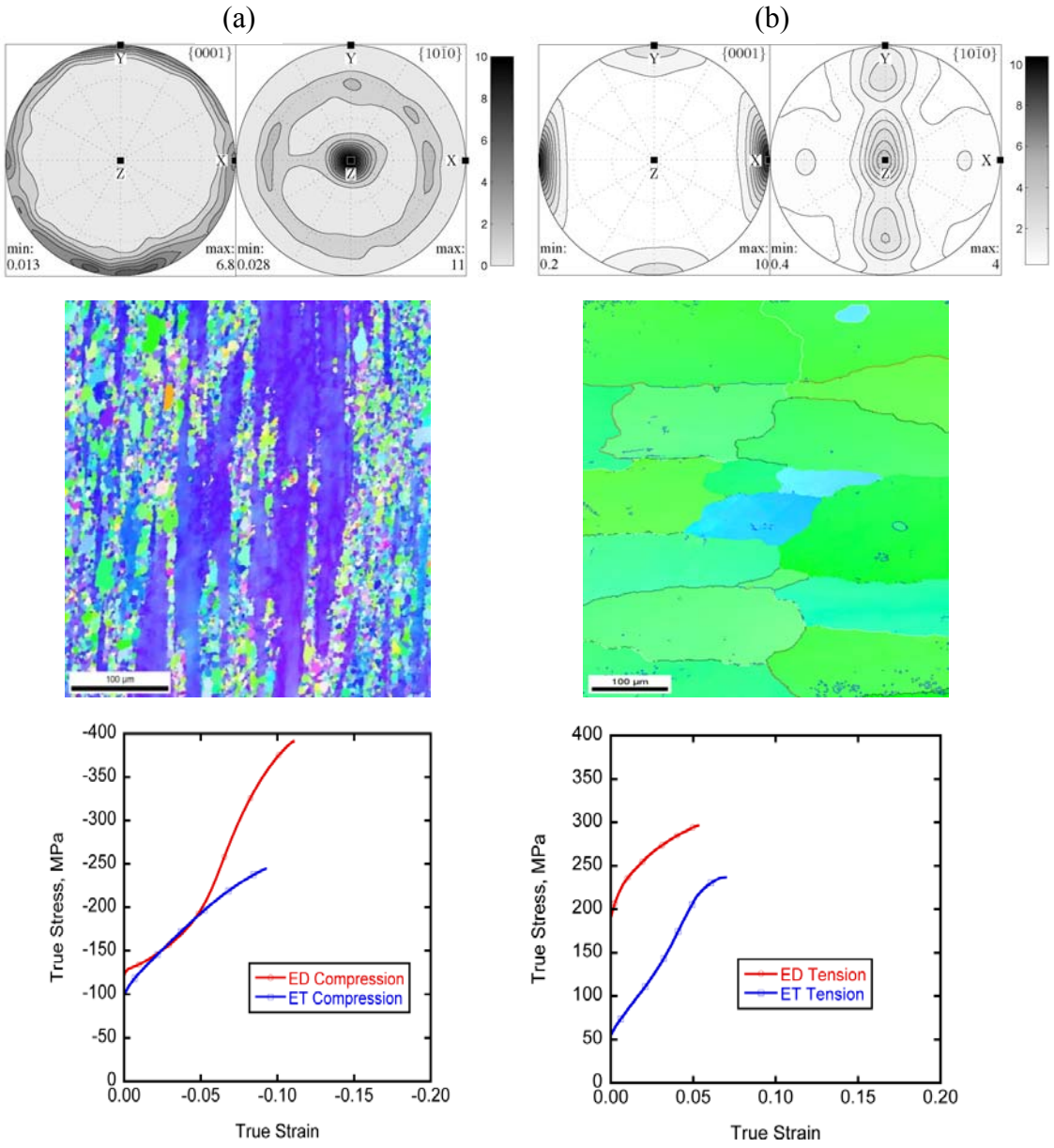


Figure 4.1 Complete (0001)&(10$\bar{1}$0) pole figures obtained by neutron diffraction of initial texture of a magnesium AM30 alloy revealing an (a) axisymmetric rod texture and (b) plane strain extrusion texture, where the z axis corresponds to the extrusion direction, (c) followed by their corresponding IPF maps and (d) Deformation characteristics along extrusion direction (ED) and extrusion transverse direction (ET) during compressive and tensile deformation. Sigmoidal curve & parabolic curve shows a yield stress of approx. 125 MPa & 100 MPa respectively for axisymmetric texture while sigmoidal curve & parabolic curve shows a yield stress of approx. 50 MPa & 200 MPa respectively for plane strain extrusion texture.

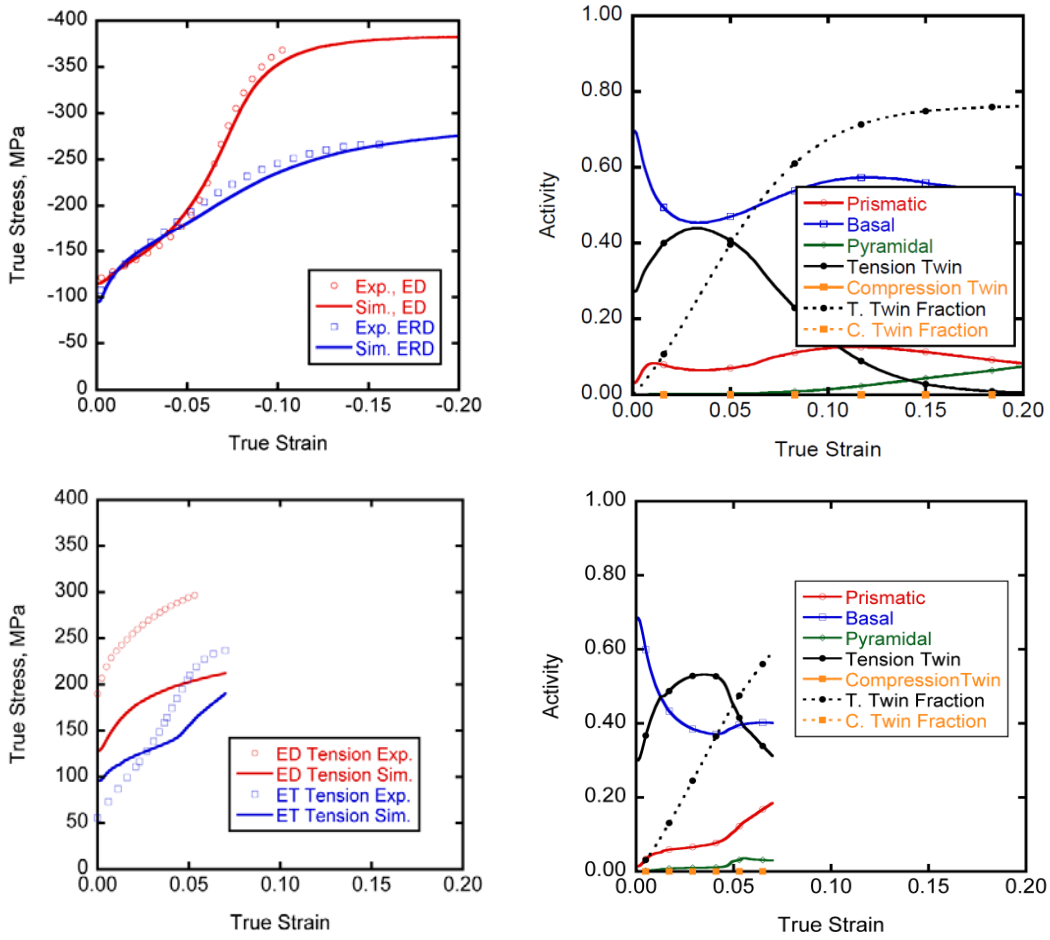


Figure 4.2 Measured and predicted flow behavior for an extruded AM30 Magnesium alloy loaded in compression along the extrusion direction (ED) and along extrusion transverse direction (ET) and corresponding relative activity of deformation modes showing results for (a) axisymmetric texture indicates a perfect fit, and (b) plane strain extrusion (spotty) texture indicates a bad fit using crystal plasticity model (by Andrew Oppedal, Crawford Baired).

For the axisymmetric texture, a perfect fit was observed using the crystal plasticity parameters but for the plane strain (or spotty) texture, simulation revealed a bad fit for the stress-strain response (by Andrew Oppedal, Crawford Baired). According to the previous assumptions, using the same material, crystal plasticity model should be able to predict the correct stress-strain response for any texture in regard of taking care of the Schmid's factor and it should also be able to predict the effect of texture as well but it did

not predict it. So, what we can expect from the experiment and simulation is that (1) the lower yield stress in the sigmoidal curve for the spotty textures stems from the softening of twinning by low misorientation boundaries (2) the higher yield stress in the parabolic curve for the spotty texture stems from hardening of prismatic /pyramidal slips by the low-misorientation boundaries. (3) The effect of boundary misorientation and character has an opposite effect on the threshold stresses for slip and twinning. Therefore, to analyze and reveal this failure of crystal plasticity in regard to understand the effect of texture at the microscale, non-destructive interrupted EBSD measurements were performed so as to incorporate the effect of microstructure.

### 4.1.2 Effect of Texture at Microscale: Non-Destructive Deformation

As shown in Figure 3.3, compression tests were done on the sample along extrusion direction and three regions were selected for EBSD measurements. Deformation behavior clearly reveals the difference in the stress-strain behavior for all the strain rates i.e. $10^{-5}s^{-1}$, $10^{-3}s^{-1}$ and $10^{-1}s^{-1}$ and can be attributed to the strain rate sensitivity of slip-twin interaction. As shown in Figure 3.3(b), we have observed classical three regimes, Regime 1, Regime 2 and Regime 3. In Regime 1, twin nucleation begins followed by the lengthwise growth of twins. In Regime 2, we observed hardening that might be due to transmutation, twin coarsening followed by the edgewise growth and in Regime 3, we observed softening and slip effects. Apart from this, a new regime, Regime D, has been observed in all the strain rates behavior but it is only predominant at $10^{-5}s^{-1}$. As clearly seen from the curves that regime D is strain rate sensitive as all have different slopes in that region. For $10^{-5}s^{-1}$, in regime D, the curve shows steep fall of slope after the

very first peak which can be attributed to the twin- slip competition as when the strain rate decreases, slip become more active and we observe a decreasing hardening rate.

### 4.1.3 Regime I – Twin Nucleation

The first onset of twins was observed at around 1.3% in both the samples 1 and 2. In sample 1, the twins nucleated at 1.22% while in sample 2, the twins nucleated at 1.3% as shown in Figure 4.3. All the twins primarily nucleated during compressive deformation at $10^{-5}s^{-1}$ at around 1.3% in both the samples are extension (Tension) twins $\{10\bar{1}2\}$ $<10\bar{1}1>$ as identified by their characteristic misorientation of $86.4°<1\bar{2}10>$ (Barnett, M.R., 2007a, Godet, S., et al, 2006, Wang, et al, 2007). As described in the literature (Barnett, M.R., 2007a), in polycrystals, the extension twins are activated during the deformation of randomly textured materials with the uniaxial compression applied along the extrusion direction or along the direction perpendicular to the c-axis. This shows that twinning involves a very large change in the initial orientation of a grain as before twinning, all the c-axis are perpendicular to the compression direction but after that, all the c-axis becomes parallel to the compression direction.

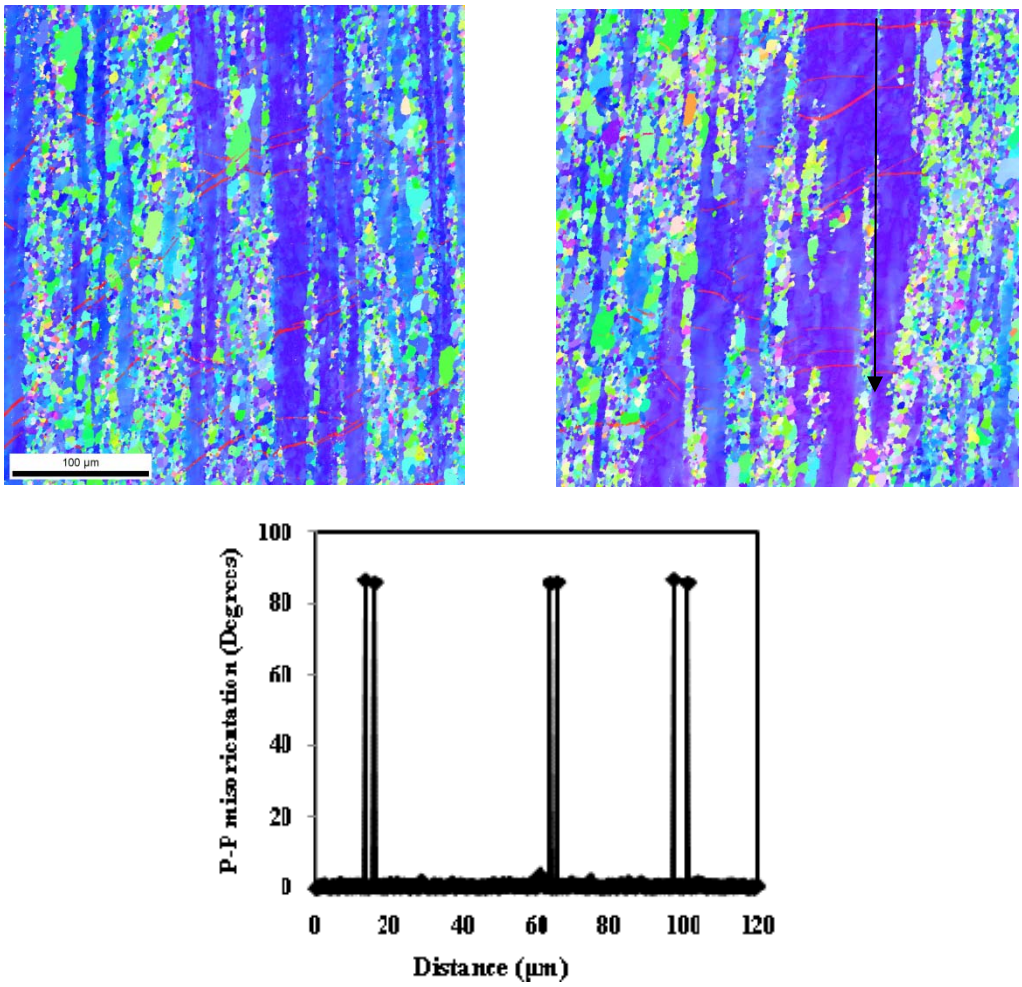


Figure 4.3 Inverse pole figure maps of an extruded AM30 magnesium alloy obtained by EBSD along extrusion direction (ED) for (a) Sample 1; nucleation of twins at 1.22% plastic strain (b) Sample 2; nucleation of twins at 1.3% plastic strain (c) Point to point misorientation line profile of the twins along the direction indicated by an arrow shows the average characteristic misorientation of 86.4˚. This shows all the twins nucleated are {10$\bar{1}$2} <10$\bar{1}$1> twins as identified by their characteristic misorientation of 86.4˚.

An interesting point to notice here is that twins exclusively nucleate in the parent grains only and there is no evidence of nucleation events in the dynamic recrystallized grains. Actually, we have assumed that it might be due to the Schmid's effects and to quantify this fact, Schmid's factor analysis was done for all the parent as well as dynamic

recrystallized grains as shown in Table 4.1 to verify the observed result. According to the Schmid's factor analysis, all the parent grains have high Schmid's factor values and accordingly, twinning occurs in grains that have high values of Schmid's factor but the analysis also showed that the dynamic recrystallized grains also have high values of Schmid's factor but still twining is almost non-existent in such grains. This provides a strong evidence for Non-Schmid's effects of twinning.

Table 4.1 Schmid's factors calculation for all the six twin variants analyzed in Region A Grain1, Region B Grain1, Region B Grain 2, Region C Grain1 and dynamic recrystallized Grain X that does not twin. The twin variants identified as active are marked in bold.

| Twin Variants | Region A Grain1 | Region B Grain1 | Region B Grain2 | Region C Grain1 | Grain X1 |
|---|---|---|---|---|---|
| $\{\bar{1}102\}<1\bar{1}01>$ | -0.083 | -0.055 | 0.042 | 0.000 | **0.175** |
| $\{1\bar{1}02\}<\bar{1}101>$ | 0.034 | 0.076 | 0.106 | 0.080 | **0.258** |
| $\{\bar{1}012\}<10\bar{1}1>$ | 0.073 | 0.088 | **0.256** | **0.297** | **0.209** |
| $\{\bar{1}012\}<10\bar{1}1>$ | **0.309** | **0.315** | **0.368** | **0.360** | **0.390** |
| $\{0\bar{1}12\}<01\bar{1}1>$ | -0.083 | -0.085 | 0.021 | 0.000 | -0.016 |
| $\{01\bar{1}2\}<0\bar{1}11>$ | 0.034 | 0.009 | 0.076 | 0.080 | -0.01 |

Therefore, to analyze the reason for poor twin nucleation in dynamic recrystallized (DRX) grains, misorientation distribution analysis was performed for parents and dynamic recrystallized grains as shown in Figure 4.4. The analysis showed that the parent grains have a high density of low misorientation angle grain boundaries while dynamic recrystallized (DRX) grains have high density of high misorientation

angle grain boundaries. Therefore, it can be concluded that the high density of high misoriented grain boundaries impedes twinning in dynamic recrystallized grains.

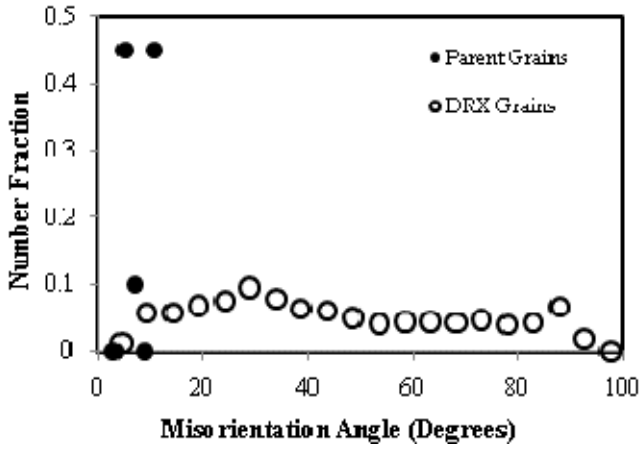


Figure 4.4 Misorientation angle distribution for parent and dynamic recrystallized (DRX) grains. The average misorientation in parent grains ~ 7.8° is less than the average misorientation in recrystallized (DRX) grains ~ 45.3°.

Also, it is found that the twin fraction is generally homogeneous at the start of twinning but some grains had substantially more twins with higher thickness than others. To quantify this observation mathematically, we plot number of twins and twin thickness vs. plastic strain as shown in Figure 4.5.

It is clearly shown in Figure 4.5 that different regions have different number of twins and consequently different twin thickness but specifically Region C has the maximum number of twins at same strain level and substantially the thickest twins. To get a clear idea of the twin morphology in Region C, EBSD generated inverse pole figure map for the region has been extended and cropped as shown in Figure 4.7.

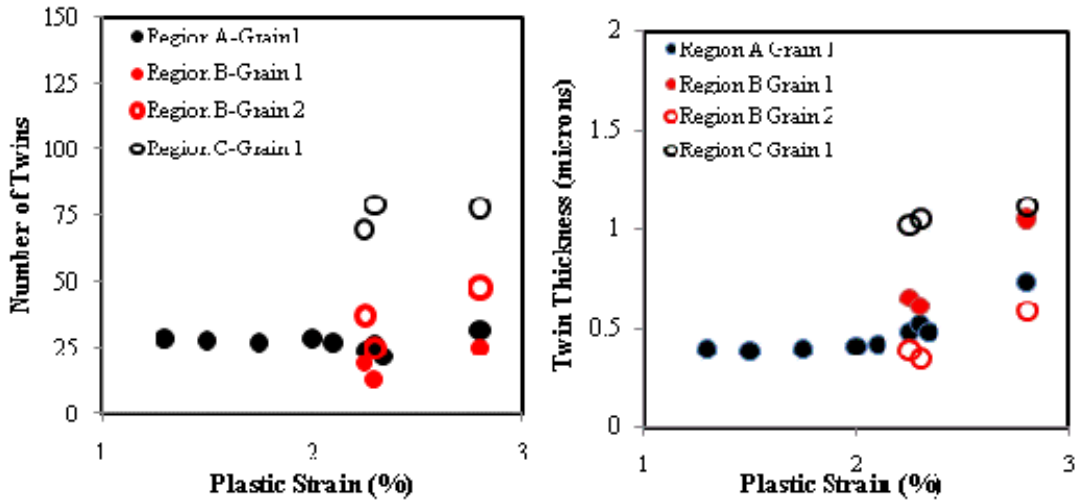


Figure 4.5 Approximate number of twins in primary observed grains and twin thickness as a function of plastic strain for all the three regions. It is clearly seen that Region C, Grain 1 has exceptionally highest number of twins and has the thickest twins.

As shown in Figure 4.7, we have observed some paired twins ( or butterfly shaped twins). These twin events indicate the travel of twin across grain boundary but actually two twin nucleation events took place along the same boundary in different grains. Such transmitted twins are actually two twins, belonging to different grains, which are joined at the approximate same position in the shared boundary. They may be either sequential twinning as when one grain terminates at a grain boundary and spark another twin in the neghbouring grain or by simaltaneous twinning when two twins nucleated from the same position in the boundary. These twin-twin events are also reported in Zr, Ti in the literature (Wang, L., et al, 2009, 2010), as a process of strain transfer across grain boundaries or the disorientation between parent grains, their size and Schmid Factor. The facts discovered by Wang et al clearly satisfy the condition here for grain boundaries where twin-twin pair nucleate as in Figure 4.4 that, the c-axis misalignment between both

the grains should be less than 25˚, the size of both the grains should be relatively large, and Schmid Factor of at least one of them should be large >0.3.

The nucleation sites for these paired twins or butterfly shaped twins are still not known but we can clearly see that these paired twins are symmetrical about one line as we can see the mirror image of these twins about a center boundary. Moreover, these paired twins are exceptionally thick and also large number of twins are nucleated in this region than the all other regions. It can be assumed that these paired twins or butterfly shaped twins nucleated at the mid-rib of the parent grain and to quantify this fact, grain boundary misorientation analysis was done and color codes were applied to the boundaries as shown in Figure 4.7.

Figure 4.6 shows distribution of misorientation angles for the three Regions A, B and C respectively for axisymmteric texture and Region E for pane strain extrusion texture. In regard to the suggested and proved results of twin nucleation at low misorientation angle in the literature (Wang, J., Beyerlein, I.J., Tome, C.N., 2010, Wang, L., Eisenlohr, P., Yang, Y., Beiler, T.R., Crimp, M.A., 2010, Beyerlein, et al, 2010), misorientation angles from 0 to 15 degress was selected and mapped to justify the above results.As we can see from the color coded boundary map that the center boundary (correspond to green color) has 5-15˚ misorientation. On further refining this boundary we found that the twins nucleated exclusively at 12-15˚ corresponding to this mid rib of the parent grain. More specifically, we observed that all the twins nucleated at the boundaries that are misoriented between 12-15 degrees. So, it can be concluded that a single, appropriately low misoriented grain boundary (12-15˚) increased the thickness (growth) and number fraction (nucleation) of twins by a factor of three so, now we have

the basis for difference in twinning stress between axisymmetric texture and spotty texture. Here, the misorientation angles in the range of upto 20 degrees are considered as low misorientation angles according to (Gjostein & Rhines, 1959).

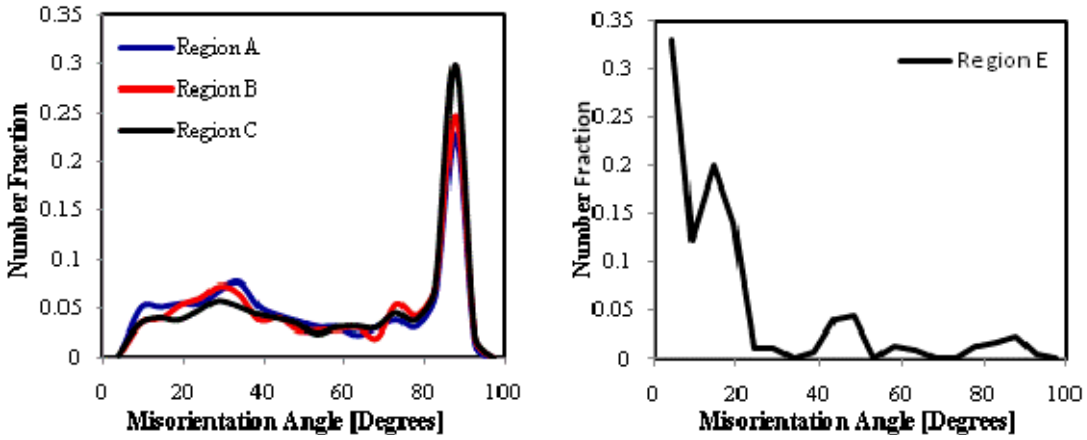


Figure 4.6 Misorientation angle distribution for axisymmetric texture and plain strain extrusion texture considering all the regions. Axisymmetric texture has high misoriented grain boundaries while plane strain extrusion texture has low misoriented grain boundaries and this difference in grain boundary misorientation justify the difference in the yield stress for both the textures.

Therefore, it can also be concluded that the reason for the difference in the yield stress between the axisymmetric texture and the plane strain texture is that the low misorientation angle favors twinning and the high misorientation angle impedes twinning.

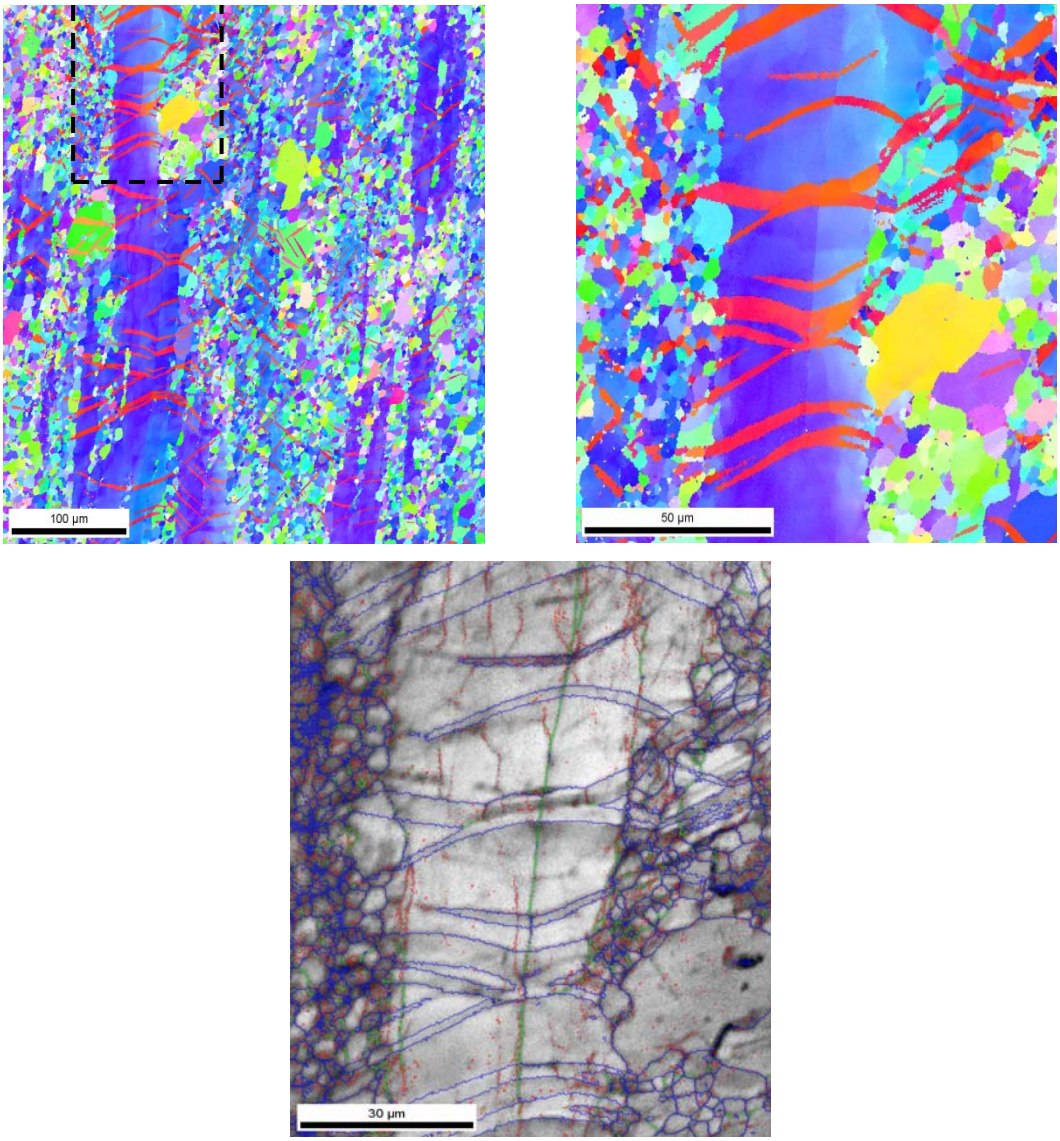


Figure 4.7 Inverse pole figure maps obtained by EBSD analysis for Region C Grain 1, cropped, shows the occurrence of some paired twins that nucleated at the middle boundary and corresponding rotation angle chart. It shows that most of the twins nucleated at low misorientation angle grain boundaries between 5˚-15˚, running across the parent grain.

## 4.2 Origin of Regime D

As shown in the hardening rate curve, there exists a decreasing hardening slope termed as Regime D. This regime also exists at higher strain rates but always neglected in the literature due to the lack of its predominance. So, in order to figure out the origin of this regime, it is correlated to the area fraction of the twins with the help of the area fraction vs. plastic strain curve as shown in Figure 4.8. Area fraction of twins was calculated using pole figure with the help of OIM analysis software by manual selection of orientations falling within some tolerance. As shown, area fraction of twins was nearly steady below 3.6% plastic strain but after that, area fractions of the twins have increased linearly with the strains. As we see in the hardening curve for $10^{-5}s^{-1}$, the very first peak corresponds to the nucleation of twins followed by the steep fall of the hardening rate. The area fraction of twins remains steady in this regime indicates that there is no further nucleation or propagation of twins takes place. The fall in the activation of twins corresponds to the activation of slip at that point when twinning stops. This halt of twin growth after noticeable nucleation can be attributed to the Regime D. The origin of this halt may correspond to a competition between non - <a> slip and twinning where slip dominates and at low strain rates pyramidal dislocation may be active. However there is an exception here for Region C as it shows a higher slope in Regime D because of the presence of the low misoriented grain boundary at the middle rib of the parent grain.

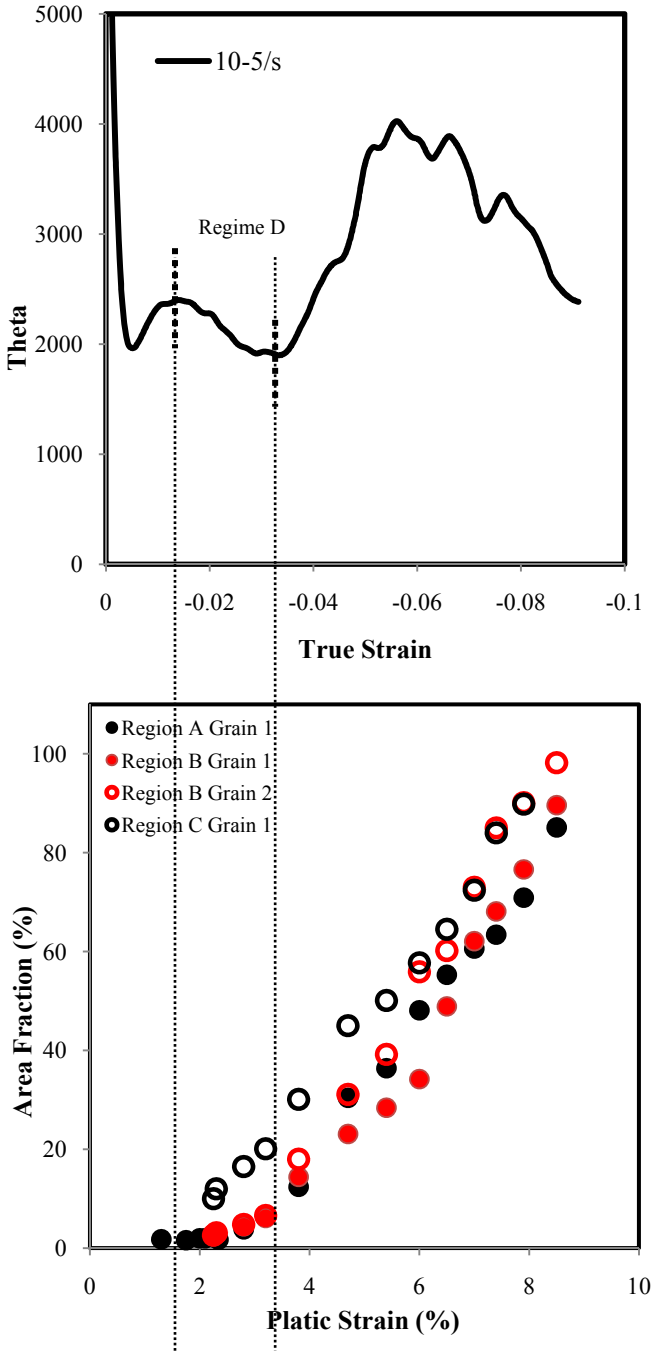


Figure 4.8 Mapping the deformation characteristics along extrusion direction (ED) at $10^{-5}s^{-1}$ (a) strain hardening rate curve and (b) measured approximate area fraction of twins in primary observed grains as a function of plastic strain for all the three regions. Regime D corresponds to the halt of twin growth after nucleation.

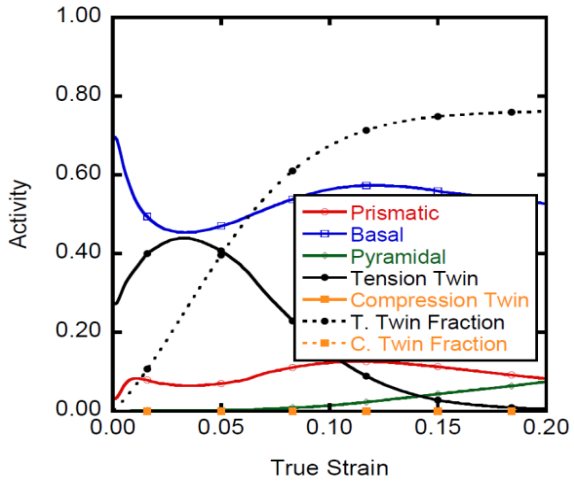


Figure 4.9 Simulated relative activity of deformation modes observed using crystal plasticity dislocation based model.

As shown in Figure 4.9, we have lots slip and twin systems active here but most predominantly prismatic and pyramidal <c+a> slip activity here. So, there might be a prismatic or pyramidal <c+a> slip activity that tries to halt the twinning. Twinning basically provides extension along c-axis during compression so, the only mode that provides c-axis strain is the pyramidal <c+a> slip as Schmid's factor is very high on it (Jiang, et al, 2007). So, we can conclude that the pyramidal <c+a> is active but it contradict the fact in the literature that it does not exists. Another observation to support this fact is that the only thing that triggers twinning is a dislocation of a burger vector that has a component along c-axis. Moreover, we know that prismatic and basal does not have c-axis component so, it should be pyramidal. So, slip substantially prevails in the competition when strain rates fall below $10^{-5}s^{-1}$. The upper bound of Regime D is approximately 3.6% and corresponds to a sudden increase in the area fractions of twins. We have also observed from the EBSD generated inverse pole figure maps from 1.35% till 3.8% plastic strain that twin activity remains constant till 3% plastic strain but

between 3% to 3.8% there is sudden increase in the activity of twins or more closely, 3.5% is the propagation threshold.

### 4.2.1 Correlation of Hardening with Transmutation Effects

As described above, number of twins increases with strain upto a certain strain level where no more new twins nucleate or grow in Regime D. As shown in Figure 4.10, we observe the number of twins vs. strain curve and found that after nucleation of twins at 1.3% plastic strain there is some drop of twins occurred before 2% plastic strain in all the regions but specifically in Region A. There is again substantial increase in twins from 2% till 4% takes place. Some difference is observed in the rate and morphology of twins nucleate in the Region B between Grain 1 and Grain 2 as shown in Figure 3.4. In Region B, Grain 1 has only one type of twins almost all progressed in same direction and same morphology but in Grain 2, there are two types of twin variants active as observed with the help of schmid factor analysis, both in different directions but has same morphology. Moreover, number of twins nucleate in Grain 2 is higher than in Grain 1 in the same Region B and some difference in the thickness of twins between both the gains was also observed. According to the theory, two phenomenons were commonly observed in this kind of behavior mainly Hall-Petch and Transmutation effects. Now, we are going to reveal transmutation effects on hardening with the help of Regime D.

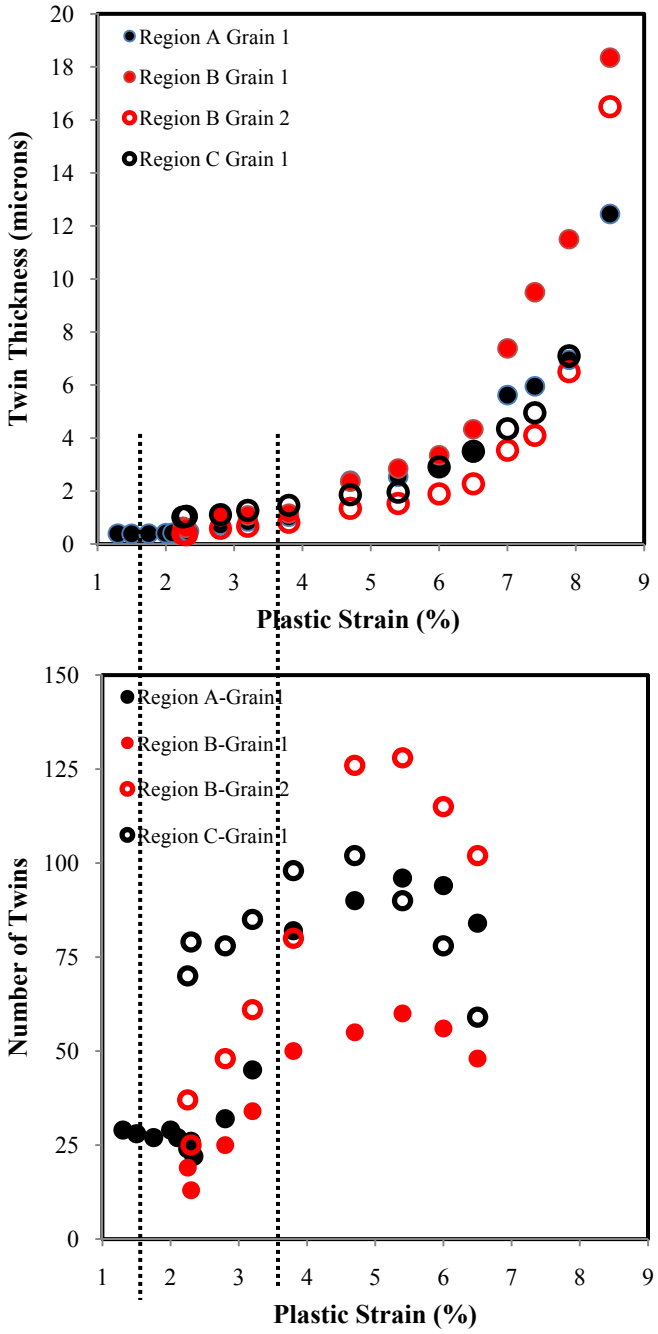


Figure 4.10 Mapping of measured approximate (a) twin thickness; shows steady thickness in Regime D (b) number of twins; shows lot of nucleation in Regime D, in primary observed grains as a function of plastic strain for all the three regions. The mapped region indicates the behavior of these curves according to regime D.

As shown, the behavior of thickness curve indicates transmutation promoting while the behavior of number fraction curve indicates Hall-Petch promoting. Regime D allows us to appreciate that it is actually transmutation that drives Regime D hardening not Hall-Petch. So, we can observe that the transmutation is driven by thickening rate while Hall-Petch is driven by nucleation rate because of low boundary misorientation. However, there are lots of nucleation events we can observe here but the twin thickness remains steady in Regime D. So, this increase in number of nucleation events and steady thickening rate can be attributed to the nucleation of new grain boundaries. As hardening rate decreases, nucleation increases so, it cannot be due to the Hall-Petch as Regime D should not be exists if there is nucleation events takes place in this regime and that clearly points out transmutation effects. So, rather than nucleation transition, transition in thickening rate is the one that drives more substantially the transition to regime II.

### 4.3 Origin of Pseudo-Elasticity

The loading and unloading behavior of magnesium and its alloys is characterized by significant strain hysteresis or Anelasticity (Mann, G.E., Sumitomo, T., Caceres, C.H., Griffiths, J.R.). As shown in the Figure 4.11, stress –strain behavior of a material illustrates the development of loading and unloading hysteresis loops. When, we load a curve and relax it, if it relaxes in a non-linear way shows the effect of Pseudo-elasticity. This non-linear response exhibit a complex problem to engineers trying to design structural components based on a constant value of the elastic modulus. Also, Pseudo-elastic strain also known as Anelastic strain (Ea) is plotted vs. measured plastic strain. Some work on AZ91, AZ31 (Mann, G.E., Sumitomo, T., Caceres, C.H., Griffiths, J.R.,

and Caceres, et al, 2003) showed that the extent of Pseudo-elastic strain is controlled by the plastic strain. The Anelastic strain was calculated mathematically with the help of observed plastic strain and young's modulus of 45 GPa. A number of studies have been conducted in the literature (Muransky, et al, 2009, Mann, et al, Caceres, C.H., Sumitomo, T., Veidt, M., 2003) on this effect but no one is sure about the origin of this non-linear unloading behavior.

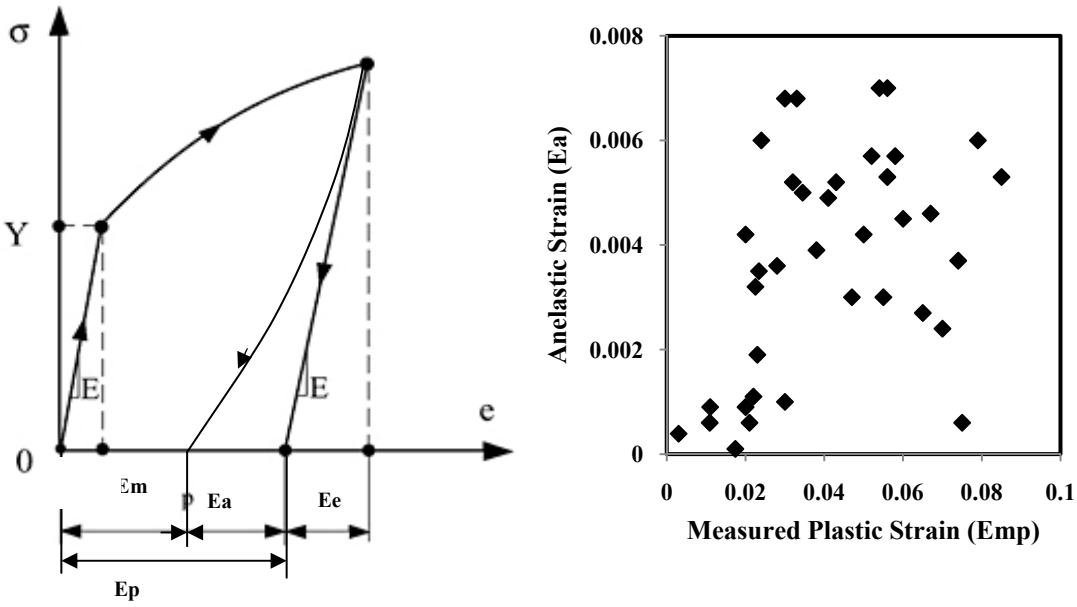


Figure 4.11 (a) Stress-Strain response followed by unloading and defining pseudo-elastic (or Anelastic strain, Ea) (b) calculation shows Anelastic strain as a function of Measured plastic strain The anelastic strain was calculated mathematically with the help of observed plastic strain and young's modulus of 45 GPa. The Pseudo-elasticity can be correlated to de-twinning on the basis of Anelastic strain curve in (b).

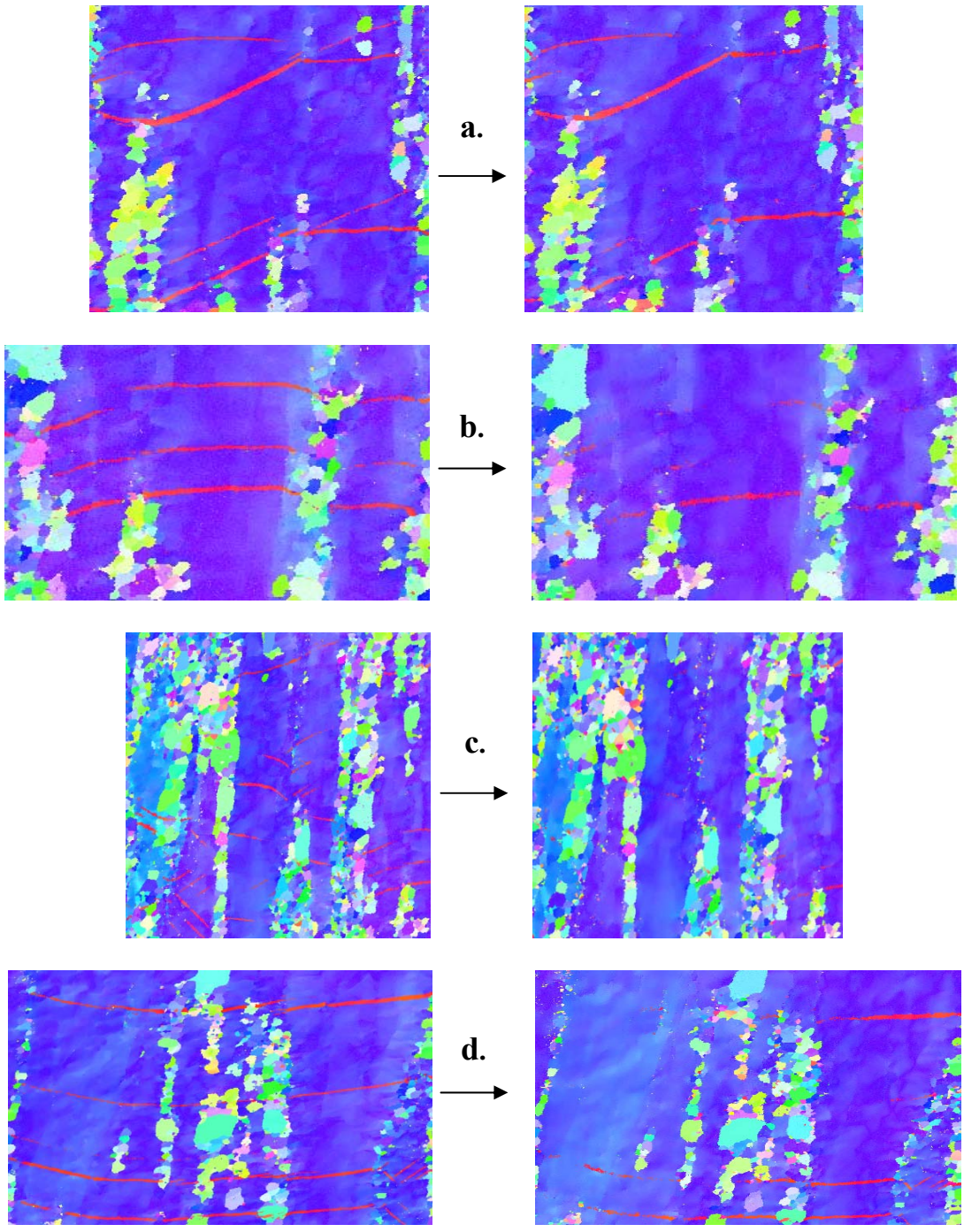


Figure 4.12 Inverse pole figure maps obtained by EBSD analysis for Region A & Region B shows appearance of twins (a) in 1.3% but disappearance in 1.5% (b) in 2.3% but disappearance in 2.34% (c) in 2.3% but disappearance in 2.34% (d) in 2.25% but disappearance in 2.3% plastic strain.

However, to study this behavior more closely, we have observed some EBSD generated inverse pole figure maps of AM30 at some strain levels as shown in Figure 4.12. We observed that some twins disappeared in the early stages of deformation at some strain level from two regions as shown and then they again re-appeared as deformation continues further and this can be correlated to this behavior. Here, we found that some twins disappear at the strain levels of 1.5%, 2.34% in region A and 2.3% in region B.

Some authors explained this on the basis of dislocation pile up mechanism during loading and when the stress is released there is de-pile up or the facts proposed by Gharghouri et al. that the Anelastic loops in magnesium are due to the elastic behavior of $\{10\bar{1}2\}$ twins, which expand as load increases and contract as load decreases. But here, this fact is contradicted by the observation based on the twin behavior that on releasing stress, twins disappear but when you again load the sample, twins does not kick back in that means complete de-twinning happened in some areas so, this indicates the proof of de-twinning before relaxation of stress. So, Pseudo-elastic behavior in magnesium is correlated to de-twinning.

As shown in Figure 4.11(b), we observed an S-shaped curve which a common behavior describing the pseudo-elastic effect, as observed in the literature by (Mann et al, Caceres, C.H., Sumitomo, T., Veidt, M., 2003). So, as can be seen here that initially we have a small plateau before plastic strain of 2% as we do not have much twinning but Pseudo-elasticity is correlated to twinning, described above, the Pseudo-elastic strain increased dramatically between 2% and 4% more exclusively at around 3.6%. As we already observed the volume fraction of twins after the halt (as shown in Regime D in

hardening rate curve) increased at 3.6% that corresponds to the increase in pseudo-elasticity strain followed by the sudden drop of this strain when twin becomes predominant as twin covers all the parent grains. Therefore, we can correlate Pseudo-elasticity with de-twinning. A double hump is also observed in the S-shaped curve at around 6% and that shows the fact that dynamic recrystallized grains starts to twin at that strain and try to increase their volume fraction as strain increases.

## 4.4 Regime II - Twin Growth

As already observed, there are different twin morphologies for different regions as shown in Figure 3.4 but an interesting thing to observe here is that Region B has different variants active in Grain 2 while only one variant is observed in Grain 1. Moreover, Grain2 has the less thick twins than Grain 1 and twins in Grain 2 evade the whole grain faster than twins in Grain 1. One more thing has to be taken into consideration that if we observe the inverse pole figure maps from 2.5% till 8%, we find that more twins nucleate in Grain 2 while in Grain 1 after a certain extent, much earlier than Grain 1, twin grows substantially in thickness. So, we have to find out among nucleation and propagation, which one is predominant in growth. The effects of twin propagation and growth have already been discussed in the literature (Wang, J., Beyerlein, I.J., Tome, C.N., 2010) in terms of hardening and texture characteristics. To quantify these observations we plot some curves as shown in Figure 4.13. As observed, twin nucleation and twin volume fraction is more in Grain 2 than Grain 1 while thickness of twins in Grain 1 increased rapidly after 4% in Grain 1 than in Grain 2. So, thickness of two variants grows very small while the thickness grows fast if we have just 1 variant and it can be expected that

the volume fraction of twins is higher in Grain 2. Also, according to the literature so far, increase in volume fraction of twins is accommodated by thickening rate. To quantify this fact, we plot nucleation rate as a function of plastic strain and found that nucleation is higher in Grain 2 and it can be concluded that nucleation contribute to the volume fraction of twins is more than the growth or thickening rate. Even the thickening rate is slow but because there is so much nuclei present in Grain 2, the volume fraction increased more. So, it can be stated that where two variants are present in a grain as in Grain 2, growth rate is faster and nucleation is more predominant than propagation. Also, Grain 1 and Grain 2 both have high Schmid's factors, one dominated by thickening and other dominated by nucleation. Also, there is a ramification what can be expected is, as observed previously, that if transmutation is accommodated by thickening rate, it will be mitigated when multi-variant twins are present because as assumed before that nucleation is attributed to Hall-Petch while growth is attributed to Transmutation.

Therefore, on the whole, it can be concluded that (a) when twin –twin interaction involves high schmid factors for both variants, twin growth is dominated by nucleation.(b) nucleation substantially mitigates thickening (c) nucleation strikingly induces more twin volume fraction increase than what would growth do by thickening. (d) This type of twin-twin interaction is then expected to reduce transmutation and such locally mitigate regime II hardening.

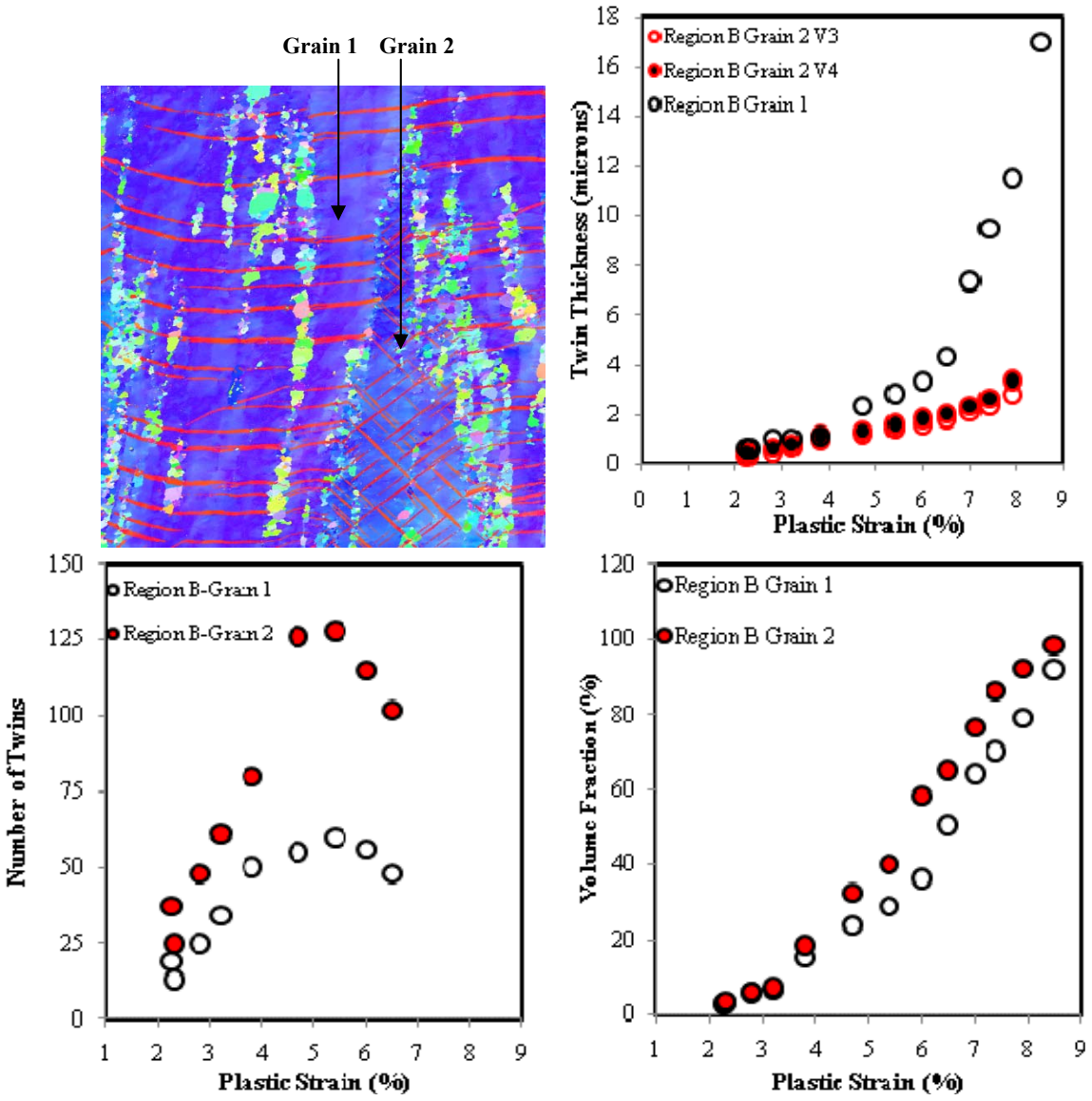


Figure 4.13 EBSD generated IPF map of Region B showing different twin variants in Grain 1 and Grain 2. Twinning activity measured in terms of (a) twin thickness as a function of plastic strain in Region B for Grain1 and Grain 2 (b) number of twins as a function of plastic strain for all the regions (c) volume fraction of twins as a function of plastic strain for all the regions. The curves indicate that nucleation contribute to the volume fraction of twins more than the thickening rate if multi variant twins are present.

# CHAPTER V

# CONCLUSIONS

This paper successfully investigate the mechanisms of twin nucleation, twin propagation, pseudo-elasticity and non-Schmid's effect in magnesium via non-destructive electron backscattered diffraction (EBSD) performed on the same region undergoing deformation with the following deliverables:

(1) Mantle effects are crucial in HCP on both twinning and non-basal slip. Aside from the Schmid factor, mantle effects should be considered to restore crystal plasticity's comprehensiveness to texture changes. In sum, low misorientation soften twinning and harden non-basal slip.

(2) A new Regime D was identified after Regime I and before Regime II, whereupon slip mitigates twinning after its first nucleation events. At very slow strain rates, the hardening rates turn to decrease dramatically in Regime D.

(3) The correlation between Regime-D's lower and upper-bounds, and the thickening rate and number fraction of twins substantiates major transmutation effects on hardening over the Hall-Petch effects.

(4) Upon multivariant twinning growing under high Schmid's factors, nucleation is strikingly more effective to increase the twin volume fraction than the growth does.

(5) Pseudo-elasticity in HCP structures is mainly due to de-twinning and thinning of residual twins not just elastic twins.

REFERENCES


Agnew, S.R., Yoo, M.H., Tome, C.N., 2001, Application of texture simulation to understanding mechanical behavior of Mg and solid solution alloys containing Li or Y, *Acta Materialia* 49, 4277-4289.

Allen, N.P., Hopkins, B.E. & McLennan, J.E., 1956. The tensile properties of single crystals of high-purity iron at temperatures from 100 to -253 degrees C. *Proceedings of the Royal Society of London. Series A. Mathematical and Physical Sciences* , 234(1197), 221.

Armstrong, R.W. & Worthington, P.J., 1973. Constitutive Relation for Deformation Twinning in BCC Metals. *Metallurgical Effects at High Strain Rates*.

Barnett, M.R., Keshavarz, Z., Beer, A.G., Atwell D., 2004. Influence of grain size on compressive deformation of wrought Mg-3Al-1Zn. *Acta Mater ialia* 52, 5093-5103.

Barnett, M.R., 2007a. Twinning and the ductility of magnesium alloys. Part I: "Tension" twins. *Materials Science and Engineering* A464, 1-7.

Bell, R.L. & Cahn, R.W., 1953. The nucleation problem in deformation twinning. *Acta Meta llurgica*, 1(6), 752–753.

Beyerlein, I.J., Capolungo, L., Marshall, R.J., McCabe, Tome, C.N., 2010, Statistical analysis of deformation twinning in magnesium, *Philosophical Magazine* Vol. 90 2161-2190.

Beyerlein, I.J., Tome, C.N., 2010, A probabilistic twin nucleation model for HCP polycrystalline metals, *Proceedings of the royal society A* 466, 2517-2544

Beyerlein, I.J., McCabe, R.J. & Tomé, C.N., 2011. Effect of microstructure on the nucleation of deformation twins in polycrystalline high-purity magnesium: A multi-scale modeling study. *Journal of the Mechanics and Physics of Solids*.

Bolling, G. & Richman, R., 1965a. Continual mechanical twinning. Part I: Formal description. *Acta Metallurgica*, 13(7), 709-722.

Bolling, G. & Richman, R., 1965b. Continual mechanical twinning. Part II: Standard Experiments. *Acta Metallurgica*, 13(7), 723-743.

Bolling, G. & Richman, R., 1965c. Continual mechanical twinning. Part III: Nucleation and dislocation production Part IV: Cyclic twinning in Fe3Be single crystals. *Acta Meta llurgica*, 13(7), 745-757.

Bristowe, P.D. & Crocker, A.G., 1977. A computer simulation study of the structure of twinning dislocations in body centerd cubic metals. *Acta Meta llurgica*, 25(11), 1363–1371.

Cahn, R.W., 1953a. Plastic deformation of alpha-uranium; twinning and slip. *Acta Meta llurgica*, 1(1), 49–52.

Cahn, R.W., 1953b. Soviet work on mechanical twinning. *I Nuovo Cimento (1943-1954)*, 10, 350–386.

Caceres, C.H., Sumitomo, T., Veidt, M., 2003, Pseudoelstic behavior of cast magnesium AZ91 alloy under cyclic loading – unloading, *Acta Materialia* 51, 6211-6218

Capolungo, L., Beyerlein, I.J., 2008, Nucleation and stability of twins in hcp metals, *The American Physical Society* 78, 024117-1 – 19

Capolungo, L., Marshall, P.E., McCabe, R.J., Beyerlein, I.J., Tome, C.N., 2009, Nucleation and growth of twins in Zr: A statistical study, *Acta Mate rialia* 57, 6047-6056.

Christian, J.W., Mahajan, S., 1995. *Deformation twinning. Progress in Materials Science* 39, 1-157.

Christian, J.W., 2002a. *The Theory of Transformations in Metals and Alloys Pergamon, p 914* , Amsterdam.

Christian, J.W., 2002b. *The Theory of Transformations in Metals and Alloys Pergamon, p 933* , Amsterdam.

Christian, J.W., 2002c. *The Theory of Transformations in Metals and Alloys Pergamon, p 953* , Amsterdam.

Cottrell, A.H. & Bilby, B.A., 1951. LX. A mechanism for the growth of deformation twins in crystals. *Philosophical Magazine Series 7*, 42(329), 573–581.

Cox, J.J., Horne, G.T. & Mehl, R.F., 1957. Slip, twinning, and fracture in single crystals of iron. *Transactions of American Society for Metals*, 118.

Godet, S., Jiang, L., Luo, A.A., Jonas, J.J., 2006, Use of Schmid factors to select extension twin varients in extruded magnesium alloy tubes, *Scripta Materialia* 55 1055-1058.

Gjostein, N. A., & Rhines, F. N. (1959). Absolute interfacial energies of [001] tilt and twist grain boundaries in copper. *Acta Metallurgica*, *7*(5), 319–330.

Harding, J., 1969. The effect of grain size and strain rate on the lower yield stress of pure iron at 288 K. *Acta Metallurgica*, 17(8), 949–958.

Harding, J., 1967. The yield and fracture behavior of high-purity iron single crystals at high rates crystals at high rates of strain. *Proceedings of the Royal S ociety of London. Series A. Mathematical and Physical Sciences*, 299(1459), 464.

Harding, J., 1968. The yield and fracture of high-purity iron single crystals under repeated tensile impact loading. *Mem Sci Rev Met*, 65, 245–254.

Huppmann, M., Lentz, M., Chedid, S., Reimers, W., 2010, Analysis of deformation twinning in the extruded magnesium alloy AZ31 after compressive and cyclic loading. *Journal of Material Science* 46, 938-950

Jain, A. & Agnew, S.R., 2007. Modeling the temperature dependent effect of twinning on the behavior of magnesium alloy AZ31B sheet. *Materials Sc ience and Engineering: A*, 462(1-2), 29–36.

Joost, W., 2010. Lightweight Materials Projects Update From DOE.

J.Koike, 2005, Enhanced Deformation Mechanisms by Anisotropic Plasticity in Polycrystalline Mg Alloys at Room Temperature, *Metallurgical and Materials Transactions* A, Volume 36A.

Jiang, L., Jonas, J.J., Luo, A.A., Sachdev, A.K., Godet, S., 2006. Twinning –induced softening in polysrystalline AM30 Mg alloy at moderate temperatures. *Scripta Mater ialia* 54, 771-775.

Jiang, L., Jonas, J.J., Mishra, R.K., Luo, A.A., Sachdev, A.K., Godet, S., 2007a. Twinning and texture development in two Mg alloys subjected to loading along three different strain paths. *Acta Materialia* 55, 3899-3910

Jiang, Lan, Jonas, John J. 2008. Effect of twinning on the flow behavior during strain path reversals in two Mg (+Al, Zn, Mn) alloys. *Scripta Materialia* 58, 803-806.

Jiang. J., Godfrey, A., Liu, W., Liu, Q. 2008, Identification and analysis of twinning variants during compression of a Mg-Al-Zn alloy, *Scripta Materialia* 58, 122-125.

Jiang, J., Godfrey, B., A., Liu, Q., 2009, Microstructure and texture evolution during warm compression of the magnesium alloy AZ31. *Science in China series E : Technology Sciences Volume* 52, 186-189.

Kelly, E.W., Hosford, W.F., 1968, The deformation characteristics of textured magnesium, *Metallurgical and Materials Transactions A*, Volume 242, 654-661.

Knezevic, Marko, Levinson, Amanda, Harris, Ryan, Mishra, Raja, K., Doherty, Roger, D., Kalindindi, Surya R., 2010, Deformation twinning in AZ31: Influence on strain hardening and texture evolution, *Acta Materialia* 58, 6230-6242

Luo, A., Alan, Sachdev, Anil, K., 2007, Development of new wrought Magnesium-Aluminum-Manganese alloy AM30, *Metallurgical and Materials Transactions A*, Volume 38A, 1184-1192.

Li, B. & Ma, E., 2009a. Atomic Shuffling Dominated Mechanism for Deformation Twinning in Magnesium. *Physical review letters*, 103(3), 35503.

Li, B. & Ma, E., 2009b. Zonal dislocations mediating twinning in magnesium. *Acta Mater ialia*, 57(6), 1734–1743.

Li, L., Zhou, J. & Duszczyk, J., 2006. Determination of a constitutive relationship for AZ31B magnesium alloy and validation through comparison between simulated and real extrusion. *Journal of materials processing technology*, 172(3), 372–380.

Mordike, B.L., Ebert, T., 2001, Magnesium – Properties, Applications, Potential, *Material Science and Engineering*, A302, 37-45.

Mann, G.E., Sumitomo, T., Caceres, C.H., Griffiths, J.R., Reversible plastic strain during cyclic loading-unloading of Mg and Mg-Zn alloys, 2007, *Material science and Engineering A* 456, 138-146.

Muransky, O.; Carr, D.G.; Sittner, P.; Oliver, E.C., 2009, In situ neutron diffraction investigation of deformation twinning and pseudoelastic-like behavior of extruded AZ31 magnesium alloy, *International Journal of Plasticity* 25, 1107-1127.

Martin, E., Capolungo, L., Jiang, L., Jonas, J.J., 2010, Variant selection during secondary twinning in Mg-3% Al, *Acta Materialia* 58, 3970-3983.

Mahajan, S., 1975. Interrelationship between slip and twinning in BCC crystals. *Acta Meta llurgica*, 23(6), 671–684.

Mahajan, S. & Chin, G.Y., 1973. Twin-slip, twin-twin and slip-twin interactions in Co-8 wt. % Fe alloy single crystals. *Acta Metallurgica*, 21(2), 173–179.

Mahajan, S. & Williams, D.F., 1973. Deformation twinning in metals and alloys. *International Materials Reviews, 18*, 43(61), 19.

Mendelson, S., 1970. Dislocation dissociations in hcp metals. *Journal of Applied Physics*, 41(5), 1893–1910.

Mendelson, S., 1969. Elastic Energy Factors for Twinning Dislocations in HCP Metals. *Journal of Applied Physics*, 40(4), 1988–1990.

Mendelson, S., 1970. Zonal dislocations and dislocation reactions with twins in HCP metals. *SCR MET*, 4(1), 5–8.

Mendelson, S., 1969. Zonal dislocations and twin lamellae in hcp metals. *Materials Science and Engineering*, 4(4), 231–242.

Meyers, M.A., V\öhringer, O. & Lubarda, V.A., 2001. The onset of twinning in metals: a constitutive description. *Acta materialia*, 49(19), 4025–4039.

Narita, N. & Takamura, J., 1974. Deformation Twinning in Ag and CuAlloy Crystals. *Phil. Mag.*, 29(5), 1001–1028.

Narita, N. & Takamura, J., 1992. Deformation twinning in fcc and bcc metals. *Dislocations in Solids*, 9, 135–169.

Patridge, P.G., The crystallography and deformation modes if hexagonal close-packed metals, *Metallurgical Reviews*

Pratt, P.L. & Pugh, S.F., 1952. Twin accommodation in zinc. *Journal Of The Institute Of Metals*, 80, 653–658.

Pratt, P.L. & Pugh, S.F., 1953. The movement of twins, kinks, and mosaic walls in zinc. *Acta Metallurgica*, 1(2), 218–222.

Price, P.B., 1961a. Nonbasal Glide in Dislocation-Free Cadmium Crystals. I. The $\{10\bar{1}2\}$ $\{\bar{1}011\}$ System. *Journal of Applied Physics*, 32(9), 1746–1750.

Price, P.B., 1961b. Nucleation and growth of twins in dislocation-free zinc crystals. *Proceedings of the Royal Society of London. Series A, Mathematical and Physical Sciences*, 260(1301), 251–262.

Price, P.B., 1960a. On dislocations loops produced by pyramidal glide in zinc crystals. In *Proceedings*. p. 370.

Price, P.B., 1960b. Pyramidal glide and the formation and climb of dislocation loops in nearly perfect zinc crystals. *Philosophical Magazine*, 5, 873–886.

Q. Ma, H. El Kadiri, A.L. Oppedal, J.C. Baird, M.F. Horstemeyer, S.C. Vogel, Twinning effects in A rod-textured AM30 magnesium alloy

Reed-Hill, R.E., 1973. Inhomogeneity of Plastic Deformation. *ASM, Metals Park, OH* , 285.

Reed-Hill, R.E., Dahlberg, E.P. & Slippy Jr, W.A., 1965. SOME ANELASTIC EFFECTS IN ZIRCONIUM AT ROOM TEMPERATURE RESULTING FROM PRESTRAIN AT 77 deg K. *Trans. Met. Soc. AIME*, 233(TID-21748).

Reid, C.N., Gilbert, A. & Hahn, G.T., 1966. Twinning, slip and catastrophic flow in niobium. *Acta Metallurgica*, 14(8), 975–983.

Robson, J.D., Stanford, N. & Barnett, M.R., 2010. Effect of particles in promoting twin nucleation in a Mg-5 wt. % Zn alloy. *Scripta materialia*, 63(8), 823–826.

Serra, A. & Bacon, D.J., 1996. A new model for $\{10\bar{1}2\}$ twin growth in hcp metals. *Phil. Mag. A*, 73, 333–343.

Serra, A. & Bacon, D.J., 1995. Computer simulation of screw dislocation interactions with twin boundaries in hcp metals. *Acta me tallurgica e t mater ialia*, 43(12), 4465–4481.

Serra, A. & Bacon, D.J., 1986. Computer Simulation of Twin Boundaries in the H. C. P. Metals. *Philos. Mag. A*, 54(6), 793–804.

Serra, A., Bacon, D.J. & Pond, R.C., 2002. Twins as barriers to basal slip in hexagonal-close-packed metals. *Metallurgical and Materials Transactions A* , 33(3), 809–812.

Serra, A., Pond, R.C. & Bacon, D.J., 1991. Computer simulation of the structure and mobility of twinning dislocations in HCP Metals. *Acta metallurgica et materialia*, 39(7), 1469–1480.

Sleeswyk, A.W., 1962. Emissary dislocations: Theory and experiments on the propagation of deformation twins in [alpha]-iron. *Acta Metallurgica*, 10(8), 705–725.

Sleeswyk, A.W., 1974. Perfect dislocation pole models for twinning in the fcc and bcc lattices. *Philosophical Magazine*, 29, 407–421.

Stanford, N. et al., 2009. Atom probe tomography of solute distributions in Mg-based alloys. *Metallurgical and Materials Transactions A*, 40(10), 2480–2487

Sung Hyuk Park, Seong-Gu Hong, Chong Soo Lee, 2010, Activation mode dependent $\{10\bar{1}2\}$ twinning characteristics in a polycrystalline magnesium alloy, *Scripta Mater ialia* 62, 202-205.

Seong-Gu Hong, Sung Hyuk Park, Chong Soo Lee, 2010, Role of $\{10\bar{1}2\}$ twinning characteristics in the deformation behavior of a polycrystalline magnesium alloy, *Acta Materialia* 58, 5873-5885

Thompson, N. & Millard, D.J., 1952. Twin formation in cadmium. *Phil. Mag*, 43, 422–440.

Venables, J.A., 1964a. In: Reed-Hill RE, Hirth JP, Rogers HC, editors. *Deformation twinning. New York: Gordon & Breach*, 77.

Venables, J.A., 1964b. The nucleation and propagation of deformation twins. *Journal of Physics and Chemistry of Solids*, 25(7), 693-700.

Vöhringer, O., 1976. Flow stress for twinning of alpha-copper alloys. *Z Metallkd*, 67(8), 518–524.

Votava, E. & Sleeswyk, A.W., 1962. Emissary dislocations in a molybdenum-rhenium alloy. *Acta Metallurgica*, 10(10), 965–970

Wang, Y.N., Huang, J.C, 2007, The role of twinning and untwining in yielding behavior in hot-extruded Mg-Al-Zn alloy, *Acta Materialia* 55, 897-905.

Wang, L., Yang, Y., Eisenlohr, P., Bieler, T., Crimp, M., D.Mason, Metall, 2009, Twin Nucleation by Slip Transfer across Grain Boundaries in Commercial Purity Titanium, *Metallurgical and Materials Transactions* 41A, 421-430

Wang, J., Beyerlein, I.J., Tome, C.N., 2010, An atomic and probabilistic perspective on twin nucleation in Mg, *Scripta Materialia* 63, 741-746.

Wang, L., Eisenlohr, P., Yang, Y., Beiler, T.R., Crimp, M.A., 2010, Nucleation of paired twins at grain boundaries in Titanium , *Scripta Materialia* 63, 827-830

Wang, J., Hirth, J.P. & Tomé, C.N., 2009. Twinning nucleation mechanisms in hexagonal-close-packed crystals. *Acta Materialia*, 57(18), 5521–5530.

Yamaguchi, M. & Vitek, V., 1976. Twin boundaries and incoherent steps on twin boundaries in body-centered-cubic metals. *Philosophical Magazine*, 34, 1–11.

Yoo, M.H., 1981, Slip, Twinning and Fracture in hexagonal close-packed metals, *Metallurgical Transactions A*, Volume 12A, 409-418.

Y.N. Wang, J.C. Huang, 2007, The role of twinning and untwining in yielding behavior in hot-extruded Mg-Al-Zn alloy, *Acta Materialia* 55. 897-905

Yang, H., Yin, S., Huang, C., Zhang, Z., Wu, S., Li, S., Liu, Y. 2008, EBSD study on deformation twinning in AZ31 magnesium alloy during quasi-in-situ compression, *Advanced Engineering Materials* 10, 955-960.

Zhang, Shaorui, Peng, Yinghong, Tang, Weiqin, Li, Dayong, 2009, The polycrystalline plasticity due to slip and twinning during magnesium alloy forming, Acta *Mater ialia* 212, 293-303.